ANNUAL REVIEWS

Annual Review of Plant Biology

Genetically Encoded Biosensors in Plants: Pathways to Discovery

Ankit Walia,[1,*] Rainer Waadt,[2,*] and Alexander M. Jones[1]

[1]Sainsbury Laboratory, Cambridge University, Cambridge CB2 1LR, United Kingdom; email: alexander.jones@slcu.cam.ac.uk

[2]Centre for Organismal Studies, Ruprecht-Karls-Universität Heidelberg, Heidelberg 69120, Germany

Annu. Rev. Plant Biol. 2018. 69:497–524

The *Annual Review of Plant Biology* is online at plant.annualreviews.org

https://doi.org/10.1146/annurev-arplant-042817-040104

*These authors contributed equally to this article.

Keywords

genetically encoded biosensors, live imaging, cell biology, calcium dynamics, FRET

Abstract

Genetically encoded biosensors that directly interact with a molecule of interest were first introduced more than 20 years ago with fusion proteins that served as fluorescent indicators for calcium ions. Since then, the technology has matured into a diverse array of biosensors that have been deployed to improve our spatiotemporal understanding of molecules whose dynamics have profound influence on plant physiology and development. In this review, we address several types of biosensors with a focus on genetically encoded calcium indicators, which are now the most diverse and advanced group of biosensors. We then consider the discoveries in plant biology made by using biosensors for calcium, pH, reactive oxygen species, redox conditions, primary metabolites, phytohormones, and nutrients. These discoveries were dependent on the engineering, characterization, and optimization required to develop a successful biosensor; they were also dependent on the methodological developments required to express, detect, and analyze the readout of such biosensors.

Contents

INTRODUCTION

In most plants, highly disparate metabolic activities occur in photosynthetic leaves, reproductive tissues, and subterranean root systems. Coordinating these activities in a dynamic environment necessitates continual mobilization of resources and information across the plant body-plan. Revealing how resources and information such as nutrients, metabolites, and signaling molecules are spatially distributed over time is thus a crucial step toward understanding how plants cope with the challenge of coordinating many cellular activities into a multicellular whole and do so in dynamic environments. Thus, there is a need to measure the levels of important molecules at physiologically relevant spatial and temporal scales and to make such measurements in vivo. Toward this end, many fields in which transgenesis is feasible have turned to genetically encoded fluorescent or luminescent biosensors to acquire high-resolution information with minimally invasive methodologies. Clearly, a lack of biosensors specific for a given analyte would limit such an approach, but an ever-growing array of biosensors is available (147). As the development and deployment of biosensors constitute an iterative process and as most extant biosensors have yet to be deployed in plants, the contribution of genetically encoded biosensors to plant biology stands to grow in the future.

Analyte: a molecule or molecular event that can be tracked with a biosensor

DEFINITION OF BIOSENSORS

Biosensor is a general term applied to many technologies to describe a molecule, organism, or device in a biological context that couples the sensing of a specific molecule of interest (analyte) or biological process to the emission of a quantifiable signal (6, 147, 165). The term *bio* can imply a biological component of the biosensor or simply that it is incorporated into a biological system (6, 147). Idealized requirements for a sensor are that it (*a*) is highly selective for a specific analyte or biological process; (*b*) enables a quantitative readout over biologically meaningful spatial, temporal, and concentration ranges; (*c*) exhibits a high signal-to-noise ratio; and (*d*) does not perturb the biological process that it measures or the biological system in which it is integrated (147, 165, 204). A broad treatment of advances in analytic techniques including mass spectrometry as well as ectopic and genetically encoded biosensors was recently published with a focus on plant hormones (145). In this article, we focus mainly on genetically encoded fluorescent biosensors and the latest achievements in plants by using such biosensors.

Direct biosensor: a biosensor that can autonomously report on analyte changes

Intrinsic biosensor: a fluorescent protein with an incorporated ligand-binding site

Extrinsic biosensor: a fluorescent protein with an attached ligand-binding site

Redox-sensitive green fluorescent protein (roGFP): a GFP-based indicator for the cellular glutathione redox status

Förster resonance energy transfer (FRET): nonradiative energy transfer from a donor to an acceptor fluorescent protein that happens over short distances

GENETICALLY ENCODED FLUORESCENT BIOSENSOR TYPES

Genetically encoded fluorescent biosensors generally consist of a sensory module coupled to fluorescent proteins (FPs) that are detected by fluorescence microscopy (165). On the basis of their biochemical properties and requirements for interactions with the cellular environment, genetically encoded fluorescent biosensors are categorized into either indirect, typically irreversible biosensors that require additional cellular components to report on an analyte or direct, typically reversible biosensors that function independently of the cellular environment (111, 192). According to this definition, a recombinant direct biosensor can also monitor analyte concentration changes in vitro, whereas an indirect reporter cannot. Examples for indirect reporters are transcription-, degradation-, and translocation-based reporters or reporters that consist of more than one molecule. The first direct biosensors were developed two decades ago to monitor cellular [Ca^{2+}] (127, 156).

Genetically encoded fluorescent biosensors are further categorized on the basis of the properties of their sensory module and attached FPs. If the FP by itself senses the analyte, it can be considered an intrinsic biosensor (147), whereas a chimera of FPs fused to a sensory module that is derived from another protein or proteins (147) is considered an extrinsic biosensor. A sensory module is not necessarily a polypeptide sequence; it could also be encoded in a nucleotide sequence, for example, in transcriptional reporters.

Another categorization of genetically encoded fluorescent biosensors is based on the number of incorporated FPs and whether the fluorescent readout is intensiometric or ratiometric. Single-FP biosensors are generally intensiometric with one excitation (Ex) and one emission (Em) maximum. However, single-FP biosensors can also be ratiometric when the FP has two excitation wavelengths that respond differentially to an analyte, for example, the pH-sensitive ratiometric pHluorin (124) and redox-sensitive green fluorescent proteins (roGFPs) (75). Alternatively, singe-FP ratiometric biosensors can exhibit two emission readouts that respond differentially to an analyte (76, 211). Double-FP biosensors also enable a ratiometric readout when the two FPs respond differentially to an analyte (65) or, as in Förster resonance energy transfer (FRET)-based biosensors, when the two FPs form a FRET pair and the amount of energy transfer responds to an analyte. FRET-based biosensors have typically harbored a cyan FP (CFP) and yellow FP (YFP) variant that function as a FRET pair with a ratiometric readout calculated from $(Ex_{CFP}Em_{YFP})/(Ex_{CFP}Em_{CFP})$ (147, 192). Recently, a new type of ratiometric genetically encoded fluorescent biosensor has been designed on the basis of dimerization-dependent FP (ddFP) exchange (5, 52). In the following, we describe

in more detail the principles of different genetically encoded fluorescent biosensor types and give an overview of what has been learned from biosensor-based approaches in plant systems.

Indirect biosensor: a biosensor that requires additional cellular components to report on analyte changes

INDIRECT BIOSENSORS

Synthetic or native hormone responsive promoters or promoter motifs have been successfully used as an indirect readout for hormone signaling strength in vivo (198, 204). For example, the synthetic *DR5* and *DR5v2* promoters driving β-glucuronidase or FPs report on the transcriptional response to auxin accumulation (113, 191). These reporters have been widely and successfully used to advance our understanding of auxin signaling dynamics in plant cells during plant development and environmental responses (24, 79, 113, 150, 164, 186, 191, 204).

A similar promoter-reporter approach was used to explore the dynamics of cytokinins [*TCS::GFP* and *TCSn::GFP* (23, 67, 136, 213)], ethylene [*EBS::GUS* (184)], and abscisic acid (ABA) (56, 214, 215). One primary limitation of transcriptional reporters such as *DR5* and *TCS::GFP* is that they report the output of the hormone signaling pathway rather than the actual hormone content within a cell. Thus, the final output can vary with changes in the components of the corresponding signaling pathway and may be affected by cross talk from other pathways. Furthermore, there is often a temporal lag between the induction of the transcriptional reporter and the initial signaling event, reflecting the time needed for transcription, translation, and reporter protein maturation. The time interval can be significantly improved by using fast-folding versions of GFP (such as the YFP variant VENUS) or luciferase as reporters (68, 175). For example, use of *DR5::VENUS* has revealed changes in auxin signaling during many developmental contexts, such as development of primordia in the shoot apical meristem (79) and stomatal development (110). Despite the caveats inherently associated with their use, promoter-reporter analyses have been instrumental in understanding many physiological and developmental processes upstream and downstream of plant hormone distributions.

FPs fused to signaling components can also be used as biosensors. Because tracking their dynamics, e.g., localization or protein degradation, does not involve or require de novo transcription and translation, these reporters can exhibit improved temporal resolution and reduced potential for cross talk from other signaling pathways compared with transcriptional reporters. For example, changes in BZR1-CFP localization have been used to reveal spatiotemporal brassinosteroid signaling in *Arabidopsis* roots and hypocotyls (33, 157). The localization of NIN-Like Protein7 (NLP7-GFP) is regulated by nitrate through a nuclear retention mechanism in *Arabidopsis* and thus can report indirectly on nitrate levels (119). Dynamics of phospholipids that play an important role in plant development as well as in mediating abiotic and biotic stress responses (138) have also been monitored through localization-based reporters (181, 193, 194).

Protein degradation–based reporters have also been used widely in plants, starting with GFP-DELLA fusion proteins whose stability is inversely responsive to the phytohormone gibberellin (GA) (139). This signaling event has been used to indirectly monitor GA levels through tracking the fluorescence of GFP-RGA (repressor of ga1-3) fusion protein (1, 51, 180). Although GFP-RGA is more stable compared with endogenous and untagged AtRGA (54), GA-induced cell elongation in hypocotyl cells is preceded by a reduction in GFP-RGA levels (168). By contrast, an increase in GFP-RGA levels occurs in hypocotyls during photomorphogenesis (2), where light-induced signals inhibit GA and hypocotyl growth.

A major advance in auxin biology was the development of the novel biosensor DII-VENUS reporter system, in which the FP VENUS is coupled with the degron motif of AtIAA28 (30). DII-VENUS biosensor fluorescence levels are inversely correlated to endogenous auxin levels, and the biosensor has been used to map auxin distribution with cellular resolution during various developmental processes (15, 16, 30, 110). A Jas9-VENUS biosensor that is degraded in the presence

of jasmonic acid (JA) was used to map local changes in JA levels in *Arabidopsis* roots and revealed two distinct phases of JA accumulation in the root upon wounding of cotyledons (108). Whereas GFP-RGA, DII-VENUS, and Jas9-VENUS are intensiometric degradation-based reporters, a ratiometric version of DII-VENUS was developed in which plants express both the auxin-sensitive DII-VENUS and a stable mDII-tdTomato (113). This R2D2 biosensor has been applied to indirectly measure auxin levels during seed development (59) and root elongation (17). Another ratiometric degradation-based biosensor, StrigoQuant, was engineered by linking AtSMXL6 with a firefly luciferase to monitor the strigolactone (SL)-sensitive degradation of AtSMXL6. Inclusion of a normalization element in renilla luciferase that is not SL sensitive was used to allow a ratiometric readout. In StrigoQuant, both SM-firefly and renilla luciferase were engineered on a single construct separated by a self-processing 2A peptide that allowed for cotranslation and cleavage from a single transcript (166). *Arabidopsis* protoplasts transiently expressing StrigoQuant were used to monitor the changes in ratio upon treatment with a synthetic strigol-like SL analog (*rac*-GR24). They also provided quantitative insights into the stereochemistry of SL perception that have relevance at the level of receptor complex formation and initiation of the SL signaling cascade.

Ratiometric pHluorin/phGFP: a green fluorescent ratiometric pH indicator

pHusion: a ratiometric pH indicator based on the fusion of eGFP with mRFP1

ClopHensor: a dual-excitation and triple-emission indicator for chloride and pH

Genetically encoded calcium indicator (GECI): a protein that changes its fluorescence properties upon binding to calcium ions

DIRECT INTRINSIC BIOSENSORS

Intrinsic biosensors harbor modifications within the FP to make them sensitive to an analyte (147). pH-dependent excitation and emission properties are intrinsic features of FPs (147), and several FPs have been engineered to monitor cellular pH changes (22, 66). Ratiometric pHluorin/phGFP is a dual-excitation (395 nm and 475 nm) and one-emission (508 nm) biosensor with a pK_a of 6.9 (124, 133, 169). For phGFP, 395-nm excitation increases and 475-nm excitation decreases with increasing pH (124). An alternative to phGFP is Pt-GFP from the organism *Ptilosarcus gurneyi*, which is a dual-excitation (390 nm and 502 nm) and one-emission (508 nm) biosensor with a pK_a of 7.3 (169). For Pt-GFP, however, 390-nm excitation decreases and 502-nm excitation increases with increasing pH (169). The rather neutral pK_a of phGFP and Pt-GFP makes them best suited for pH measurements in the cytoplasm. To monitor pH changes in a more acidic environment, researchers designed the dual-excitation and dual-emission pH biosensor pHusion (pK_a of 6). It consists of an mRFP1-eGFP tandem FP pair, where eGFP is the pH-sensitive moiety (65).

The pK_a of YFP is dependent on the concentration of halide or nitrate ions, and at pH 7, YFP fluorescence decreases with increasing concentrations of chloride or nitrate, making it suitable as a halide biosensor (90, 200). On the basis of these findings, YFP-H148Q variants have been generated with improved anion sensitivities for iodide, chloride, and nitrate (61). Through the fusion of chloride-sensitive YFP to the insensitive CFP, a ratiometric FRET-based chloride biosensor termed Clomeleon was developed (104). ClopHensor (E^2GFP fused to mDsRed) is a triple-excitation and dual-emission biosensor in which 458-nm excitation of E^2GFP is pH independent, 488-nm excitation of E^2GFP is pH dependent, and 543-nm excitation of mDsRed is pH and chloride independent, making ClopHensor suitable for simultaneously assessing pH and chloride concentration changes (11). Beyond intrinsic pH and halide sensitivity, FPs have also been engineered either to enhance intrinsic sensitivity in or to introduce intrinsic sensitivity to metals (34, 158), redox conditions (rxYFP and roGFP) (75, 149), and calcium (CatchER) (187).

DIRECT EXTRINSIC BIOSENSORS: CALCIUM INDICATORS AS PROTOTYPES

The possibilities for designing direct extrinsic fluorescent biosensors can be best illustrated by the development of genetically encoded calcium indicators (GECIs). The development of the

first GECIs two decades ago initiated the advent of direct biosensors. Since then, more than 40 fluorescent GECIs have been described (154), and the numbers are steadily increasing (**Figure 1**). Today, fluorescent GECIs are the most advanced and widely adopted direct fluorescent biosensors.

Circularly permutated fluorescent protein (cpFP): a fluorescent protein in which the N and C termini have been linked and new termini created

GCaMP: a green fluorescent calcium indicator based on the fusion of the M13 peptide with cpGFP and calmodulin

Yellow cameleon: a calmodulin- and M13-based calcium indicator that uses FRET as quantitative readout

GECO: genetically encoded calcium indicator for optical imaging

Two early design strategies for direct GECIs continue to be widely applied. These are single-FP intensiometric biosensors (14, 141, 143) and double-FP ratiometric FRET-based biosensors (127, 156). Single-FP GECIs use FPs that are split at a certain position (between amino acids 144 and 145 for GFP) and in which their original N terminus is fused to the C terminus via a short flexible linker (14). Fusion of sensory modules to such circularly permutated FPs (cpFPs) with altered FP topology can have a profound effect on FP fluorescence. This principle has been used to design two types of cpFP-based GECIs that are dependent on the insertion site of the sensory module. In Camgaroos, the calcium-binding calmodulin (CaM) was inserted between the cpFP fragments (14, 69); in Pericams and GCaMPs, the CaM-binding M13 fragment from myosin light-chain kinase (M13) was fused to the N terminus, and CaM was fused to the C terminus of the cpFP (141, 143). GCaMPs have been extensively engineered to improve their signal-to-noise ratio and calcium-binding properties (4, 40, 185, 190). However, the latest achievements based on the GCaMP design include single-FP GECIs that emit fluorescence at different wavelengths (3, 211) or that enable photoactivation/photoconversion (25, 60, 82).

Double-FP ratiometric GECIs are typically FRET-based and grouped into three different classes. These are the yellow cameleons (127), the FIP-CA (fluorescence indicator protein for Ca^{2+}) indicators (156), and troponin C–based biosensors (78, 118, 188). In yellow cameleons, the calcium-binding CaM-M13 sensory module was inserted between N-terminal eCFP (enhanced cyan FP) as the FRET donor and C-terminal eYFP (enhanced yellow FP) as the FRET acceptor (127). Another configuration was used for FIP-CA indicators, in which the M13 peptide linked both FPs and CaM was located at the C terminus (156). Cameleons and troponin C–based biosensors were both committed to several rounds of improvements, including the use of cpFPs as FRET acceptor (142), a redesign of the sensory module to reduce perturbation of cellular components (151), and the modification of the CaM-M13 linker to increase their calcium affinity (83).

Researchers have also developed a new design for ratiometric GECIs based on ddFPs (52). A ddFP consists of a monomer (copy A) that contains a chromophore and a monomer (copy B) that does not form a chromophore but increases the fluorescence of copy A after AB heterodimer formation. Copy B can form heterodimers with green A or red A copies to form functional green or red ddFPs. The ddFP-based GECI is a combination of all three monomer copies that are linked via red A-CaM-B-M13-green A (52). According to the calcium-dependent structural conformation of the CaM and M13 domains, the B copy forms a functional ddFP with either the green A or red A copy, resulting in calcium-dependent changes in the red/green emission ratio. The ddFP-based biosensor design opens new possibilities and has been applied to monitor various biological processes (5, 6, 52).

Single-FP GECIs exhibit higher signal-to-noise ratios compared with FRET-based GECIs (154). However, at high magnifications and during prolonged imaging, ratiometric biosensors are preferred because they are internally normalized and can compensate for small focal drifts or variations in GECI concentrations (146). To combine the high signal changes of single-FP GECIs with a ratiometric readout, a reference FP was fused to single-FP GECOs and GCaMPs (41, 55, 199) or the reference FP LSSmOrange was inserted within the cpFP of GCaMP6s (13) (**Figure 1**).

CHOICE OF THE RIGHT BIOSENSOR VARIANT AND DESIGN

The huge number of GECIs not only illustrates the variety of biosensor designs but also indicates why so many GECIs are needed and how some are better for certain experiments. Efforts

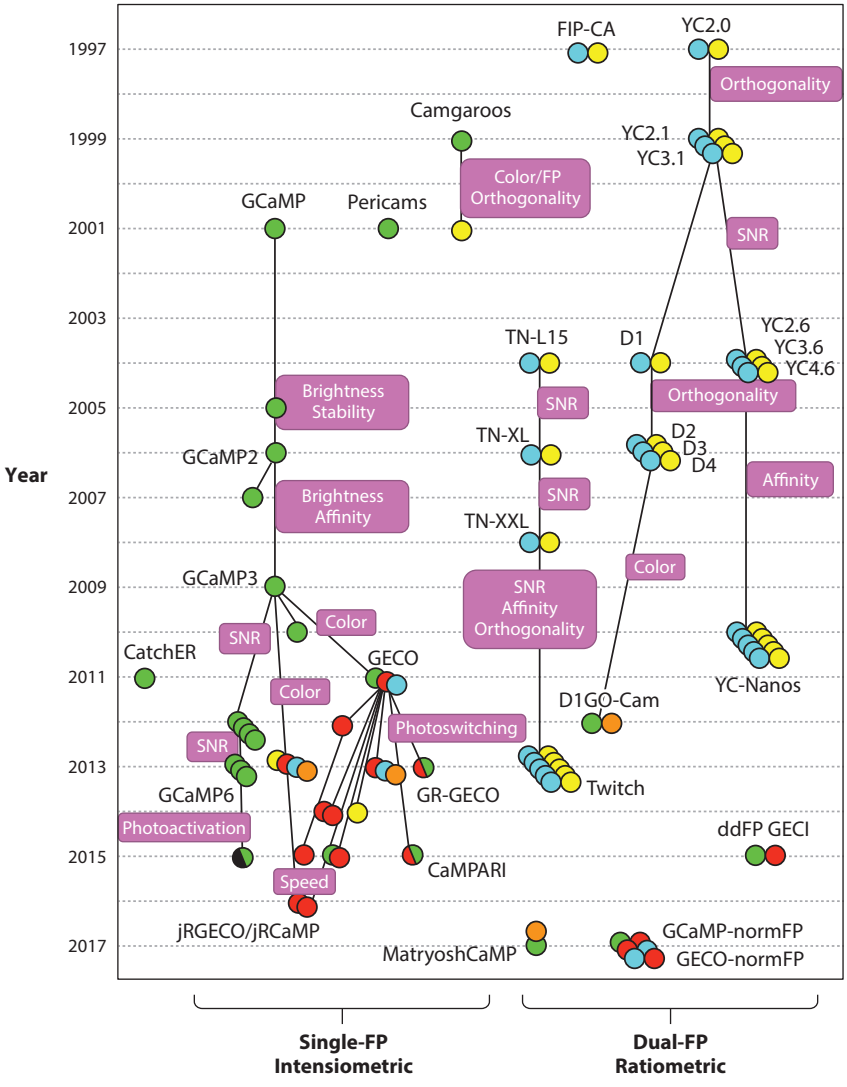

Figure 1

Evolution of GECIs over the past 20 years. Biosensors are plotted per year of their publication, with dots colored according to the emission wavelength of their constituent FPs: (*left*) single-FP biosensors and (*right*) double-FP biosensors. Purple boxes highlight new attributes for each biosensor. Abbreviations: CaMPARI, calcium-modulated photoactivatable ratiometric integrator; CatchER, Ca^{2+} sensor for the endoplasmic reticulum; D1GO-Cam, green-orange cameleon; ddFP, dimerization-dependent FP; FIP-CA, fluorescence indicator protein for Ca^{2+}; FP, fluorescent protein; GCaMP, GFP calmodulin M13 peptide; GECI, genetically encoded calcium indicator; GECO, genetically encoded Ca^{2+} indicators for optical imaging; GR-GECO, green red GECO; MatryoshCaMP, GCaMP with normalization FP nested within sensory FP; normFP, normalization FP; SNR, signal-to-noise ratio; TN-L15, troponin C with N terminus at leucine 15; YC, yellow cameleon.

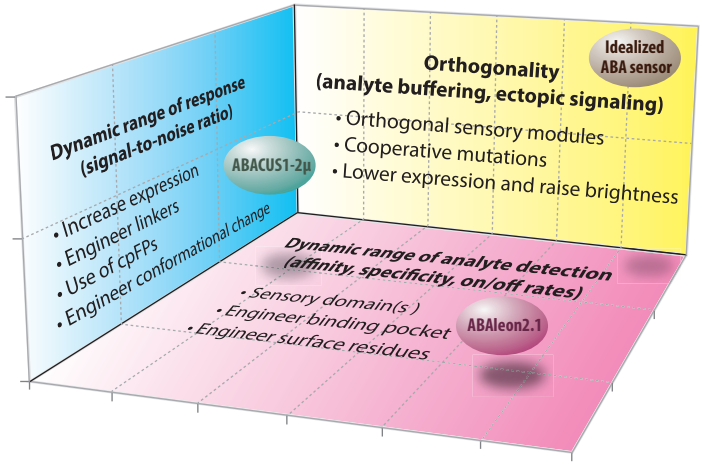

Further considerations:

- Color (imaging, autofluorescence, multiplexing)
- Brightness
- Expression in vivo (silencing, cell types)
- Subcellular localization
- Intensiometric versus ratiometric
- In vivo control sensors
- Imaging modality
- Image analysis

Figure 2

Biosensor considerations. Successful engineering and use of genetically encoded biosensors relies on appropriate consideration of the key parameters diagrammed. For example, the contrasting features and limitations of current ABA biosensors [ABACUS1–2 µ and ABAleon2.1 (92, 197)] as well as an idealized ABA biosensor are plotted. An idealized biosensor should display high dynamic range of biosensor response, a dynamic range of analyte detection that is physiologically relevant, and high orthogonality. Abbreviations: ABA, abscisic acid; ABACUS, abscisic acid concentration and uptake sensor; cpFP, circularly permutated fluorescent protein.

to improve GECIs followed the goals to increase signal-to-noise ratio, modify binding affinity, improve binding kinetics, decrease buffering capacity, make GECIs less invasive, and enable subcellular analyses and multicolor approaches (**Figure 2**). Generally, using the latest biosensor versions is recommended, as they likely exhibit improved properties. However, the choice of the right biosensor depends on the available microscopic setup and experimental requirements (154, 162). Especially for subcellular analyses, certain biochemical requirements need to be considered. Analyte concentrations, pH, autofluorescence, and tissue geometry can vary between different cellular compartments and tissues. To enable reliable and adequate analyses, the analyte-binding affinity of the biosensor should be close to the steady-state analyte concentration in the respective compartment. Most FPs are sensitive to acidic environments (174, 175). Therefore, the pK_a of a chosen FP should not match the compartment pH unless monitoring of pH is desired (175). Plants contain many fluorescent compounds (64); therefore, investigators should opt for FPs whose excitation and emission can be spectrally separated from the autofluorescent compounds that are present in the imaged compartment.

Different configurations and biosensor designs provide some flexibility for the design of novel direct biosensors, although having an idea about a potential sensory module is necessary. If a three-dimensional structure of the sensory module is available, a cpFP- or FRET-based biosensor configuration should be chosen depending on the structural orientation of the sensory module N and C termini. Because further development is largely empirical (147), screening technologies using a high combinatorial space of sensory module variants and FRET pairs (92) can aid the

identification of candidate biosensors for further optimization. Optimization strategies can be either structure guided and then followed by random site-directed mutagenesis (4, 190) or guided by large screenings of mutant biosensor libraries (114, 155, 211). Recently, a novel strategy for the identification of cpFP insertion sites into sensory modules was described (140). In this approach, cpGFP was randomly inserted into maltose-binding protein by using a transposon-based cloning strategy and subsequent fluorescence-activated cell sorting and next-generation sequencing. Through the use of next-generation sequencing, Nadler et al. (140) were able to provide a comprehensive view of hot spots for insertion sites.

BIOLOGICAL DISCOVERIES MADE WITH BIOSENSORS

Calcium Imaging

Calcium is an important signaling molecule that mediates multiple physiological and developmental processes and exhibits rapid fluctuations in concentration in a variety of subcellular compartments (53, 103). To date, biological findings that report using fluorescent GECIs in plants have been described in approximately 80 publications. Here, we focus on a subset of important and latest findings generated with fluorescent GECIs.

Calcium Imaging in Guard Cells

Calcium imaging in plants using FRET-based yellow cameleons has been pioneered through work performed in guard cells (9). In guard cells, yellow cameleons display spontaneous cytoplasmic calcium oscillations as well as calcium oscillations that are triggered or modulated via external applications of calcium, ABA, MeJA, H_2O_2, sorbitol, yeast elicitor (YEL), chitosan, allylisothiocyanate, flg22, chitin, and changes in [CO_2] (7–9, 85, 93–95, 115, 153, 189, 209, 210). Calcium transients in guard cells can be artificially imposed via alternate perfusions with hyperpolarizing and depolarizing buffers (7). With such a system, the optimal calcium pattern for stomatal closure was defined by three 5-min transients at periods of 10 min (7).

A challenge in guard cell calcium-signaling research has been identifying guard cell plasma-membrane calcium-permeable (I_{Ca}) channel-encoding genes that are activated by ABA, H_2O_2, MeJA, YEL, and chitosan (73, 95, 137, 153). Studies using yellow cameleons have contributed to the characterization of mutants mediating such calcium responses via I_{Ca} channels. For example, the *gca2* mutant failed to activate I_{Ca} channels in response to H_2O_2 (153) and showed altered calcium patterns in response to external calcium, ABA, and CO_2 (7, 209). Plants with mutations in the calcium-dependent protein kinase *CPK6* were impaired in generating ABA-, MeJA-, and YEL-induced calcium transients and in activating I_{Ca} channels (132, 137, 208). *AtrbohD/AtrbohF* double mutants with reduced reactive oxygen species (ROS) production were impaired in mediating ABA-induced calcium transients and activation of I_{Ca} channels in guard cells, but they responded to H_2O_2 (105). These findings point to the interdependence of calcium, ABA, and ROS signaling in guard cells. The interdependence of ABA and JA signaling was highlighted by the findings that the ABA synthesis mutant *aba2-2* was suppressed in MeJA-induced calcium transients but responded to ABA (84). Beyond I_{Ca} channel activity, the use of yellow cameleons also contributed to the characterization of a potential role for vacuolar calcium sequestration (8) and plastidic calcium sensing in guard cell calcium patterns (74, 203).

Guard cell calcium imaging has been performed mainly on epidermal strips that were glued on glass slides (9). Recently, guard cell calcium imaging has been performed on intact leaves either with an inverted microscope to image the abaxial leaf surface while stimulating the adaxial leaf surface or with an upright microscope for simultaneous imaging and stimulation of the abaxial

leaf surface (93). Interestingly, treatments with the pathogen-associated molecular patterns flg22 and chitin indicated different calcium response patterns dependent on the imaging setup. Indeed, flg22-induced calcium oscillations in guard cells were observed on only the upright imaging setup (93). In contrast to previous studies that used yellow cameleons, this study established the red-emitting single-FP biosensor R-GECO1 to monitor cytoplasmic calcium changes in guard cells.

Calcium Imaging in Pollen Tubes and During Fertilization

Calcium imaging in pollen tubes was initially established with yellow cameleon YC2.1. For a broader overview about the role of calcium in pollen tubes please refer to References 97 and 183. In *Lilium longiflorum* and *Nicotiana tabacum*, investigators reported a calcium gradient along with tip-focused oscillations (152). During in vitro *Arabidopsis* pollen tube growth, the calcium-permeable channel cyclic nucleotide-gated channel CNGC18 (63), ROS-producing NADPH oxidases *AtRBOHH* and *AtRBOHJ* (109), and D-serine affected tip-focused calcium oscillations (71, 123). Pharmacological and genetic evidence also indicates that glutamate receptor-like channels play a role in the self-incompatibility response (87).

During in vivo pollination in *Arabidopsis*, cytoplasmic calcium is increased in pollen grains at the pollen tube germination site and oscillates in the pollen tube tip after penetration of the papilla cell wall (89). In papilla cells, cytoplasmic calcium increased during pollen hydration at the contact site with the pollen grain, after pollen protrusion, and during pollen tube penetration (89). During double fertilization, synergid cells display cytoplasmic calcium oscillations upon contact with the pollen tube tips, which also exhibit calcium oscillations. After growth acceleration, pollen tube burst induces a short calcium transient in the pollen tube tip that spreads toward the shank. Pollen tube burst also induces a short calcium transient in egg and central cells as well as rupture of the receptive synergid. Finally, another calcium transient appeared after successful fertilization of the egg cell (49, 72, 88, 144). This developmental process has been best illustrated through simultaneous visualization of calcium signals in pollen tubes with R-GECO1 and in synergids with YC3.6. As a result, investigators concluded that intercellular communications between the pollen tube and synergids coordinate their calcium dynamics and that synergids control sperm delivery through the FERONIA signaling pathway (144).

Calcium Imaging in Roots

In *Arabidopsis* roots, calcium imaging with GECIs has been performed to study responses to gravity and mechanical stimulation, cold, changes in extracellular ion compositions (K^+ and Na^+), trivalent ions (Al^{3+}, La^{3+}, and Gd^{3+}), osmotic stress, ATP, glutamate, H_2O_2, small peptides, pathogen-associated molecular patterns, and hormones (19, 28, 44, 77, 93, 101, 115, 129–131, 159, 199). Generally, these extracellular treatments induce transient and local increases in cytoplasmic calcium concentrations. However, the removal of extracellular triggers, such as the osmolyte sorbitol or K^+, through perfusion with control or depletion, depolarization, and hyperpolarization buffers also induces calcium transients (19, 101, 115). Interestingly, K^+ deficiency triggers two distinct responses: a rapid and transient calcium increase in the stelar tissue of the elongation zone and a sustained calcium elevation after 18 h in the root-hair zone (19). Furthermore, commonly used calcium channel blockers such as La^{3+} and Gd^{3+} initially induce rapid calcium transients in roots (159). Therefore, to block calcium channels with these chemicals, prolonged pretreatments are required.

Gravistimulation triggered calcium signals at the side of the root located toward the gravity vector (131). Gravitropism is tightly associated with auxin signaling (167), and auxin also induces calcium signals in the root elongation zone (131, 177, 199). The cyclic nucleotide-gated channel 14 (CNGC14) may be essential for auxin-induced calcium signals, and *cngc14* mutants are also

impaired in gravitropic responses (177). Several members of the CNGC gene family have been characterized as calcium-permeable channels (63, 202). Therefore, CNGC14 likely represents the calcium-permeable channel activated by auxin. However, the mechanism for auxin-mediated CNGC14 activation remains to be elucidated.

Local salt stress in the root induces a calcium wave that travels through the root cortex and endodermis at a speed of ~400 μm/s (44). This shoot-ward calcium wave is blocked through pretreatment with calcium channel blockers and affects salt-induced gene expression in the shoot, indicating a long-distance systemic salt stress response mediated by calcium (44). The speed of the salt-induced calcium wave is dependent on the vacuolar ion channel TPC1 and the ROS-producing NADPH oxidase AtRBOHD (44, 57), indicating that an interplay between calcium and ROS is required for long-distance calcium signal propagations (42, 183).

Calcium imaging with fluorescent GECIs has been applied not only in *Arabidopsis* but also in rice and legumes. Compared with *Arabidopsis*, calcium signals in rice display a lower signal amplitude and a greatly increased signal duration in response to glutamate and artificially imposed calcium signals (20). In legumes, GECI-based calcium imaging has been used mainly to study the symbiosis with rhizobial bacteria and mycorrhizal fungi. Rhizobial bacteria and mycorrhizal fungi induce similar calcium patterns and require the same signaling components (98, 148, 178, 179). However, the calcium patterns depend on the stage of infection: Low-frequency spiking occurs during intracellular remodeling before infection, and high-frequency spiking occurs during the initial stage of apoplastic cell entry (178). Symbiosis-induced calcium changes originate from nuclear membranes in *Medicago truncatula* root hairs and predominantly require the activity of calcium ATPase MCA8 and cyclic nucleotide-gated channels (31, 35).

SUBCELLULAR TARGETING OF GENETICALLY ENCODED CALCIUM INDICATORS

GECIs have been targeted to several subcellular compartments and membranes (46) with recent targeting of YC3.6 and YC4.6 to the chloroplast stroma (116). Targeting of GECIs into organelles may facilitate discovery of organelle-specific calcium responses. By contrast, the attachment of GECIs to the cytoplasmic side of compartment-specific membranes may increase the spatial resolution of calcium response analyses (101).

There are controversial reports on whether the endoplasmic reticulum (ER) functions as a calcium store in plants. On the one hand, GECI-based calcium imaging in the ER lumen in combination with pharmacological treatments that induced calcium depletion from the ER suggest that the pollen tube ER serves as a calcium store (86). On the other hand, imaging in roots indicates that ER calcium follows cytoplasmic calcium patterns in response to several stimuli, but with distinct ER-specific response dynamics (28). On the basis of these data, it has been suggested that the ER does not function as a source of calcium whose release contributes to cytoplasmic calcium patterns (28).

Similar to the nucleus and ER, calcium signals in peroxisomes, mitochondria, and chloroplasts follow cytoplasmic patterns with distinct response kinetics (115, 116). YC3.6 has recently been used to analyze mitochondrial calcium responses in *micu* mutants that lack a mitochondrial calcium-binding protein with homology to components of the mitochondrial calcium uniporter machinery (201). Mitochondria of *micu* mutants display increased basal calcium levels and more rapid calcium responses with higher maximum calcium concentrations in response to ATP and auxin. It has been concluded that MICU functions as a throttle to control mitochondrial calcium uptake (201).

Compared with YC3.6 expressed in the cytoplasm, chloroplast stroma–targeted YC3.6 exhibits decreased basal emission ratios in root plastids, indicating lower basal calcium concentrations (116). In response to a transition from white to low-intensity blue light, stromal calcium increases steadily, but only in green tissues and independent of extrachloroplastic calcium. Single-chloroplast calcium

imaging revealed infrequent stromal calcium spikes that depend on extrachloroplastic calcium (116).

HyPer: a ratiometric indicator for hydrogen peroxide

VISUALIZATION OF REACTIVE OXYGEN SPECIES AND REDOX CHANGES

ROS are reactive forms of molecular oxygen and are formed as toxic by-products in metabolic reactions. Yet they also act as signaling molecules to mediate metabolic, growth, and developmental processes (96, 205). ROS levels are essential for life and need to be kept above a cytostatic but below a cytotoxic level to enable proper redox biology (125). ROS levels are regulated through the concerted action of subcellular compartmentalized ROS-producing and ROS-scavenging mechanisms to maintain an optimal cellular redox state (126).

ROS and redox biosensors mainly include intrinsic probes (roGFPs and rxFPs) to monitor the glutathione redox state (2GSH/GSSG-ratio) and extrinsic biosensors for the NAD^+/NADH-ratio, H_2O_2 (HyPer-family and modified roGFPs), and other ROS (27; for a summary of early work using ROS and redox biosensors in plants, see 43). In plants, roGFPs have been used mainly to determine the subcellular glutathione redox potential (91, 163, 173) and to measure the glutathione redox state in mutants that are involved in glutathione biosynthesis (121, 122). Experiments using roGFPs were recently performed to investigate the effects of abiotic stress on organellar redox dynamics (29). Long-term treatments indicate increased glutathione oxidation in response to several stresses and some degree of organellar specificity that is dependent on the stress (29, 173). Short-term analyses of [H_2O_2] changes in *Arabidopsis* guard cells and roots have also been performed by using HyPer (21, 45, 80). Analyses indicate that H_2O_2 scavenging in peroxisomes could be stimulated via artificial calcium elevations that may trigger the activation of catalases (45).

MEASURING pH WITH pH-SENSITIVE FLUORESCENT PROTEINS

pH homeostasis is important for secondary transport processes, protein modifications and sorting, and vesicle trafficking (170). Intracellular pH gradients are established through the coordinated activity of H^+ pumps and associated ion transporters and are indispensable for cellular compartmentalization and ion homeostasis (18, 170). Work using pH-sensitive FPs in plants has been summarized previously (43, 66). Early work was performed using ratiometric pHluorin (121) optimized for plants (termed phGFP) (133). phGFP enabled the visualization of pH gradients in *Arabidopsis* roots, with more acidic pH (6.5–7) in root-cap cells, relatively alkaline pH (7.3–7.6) in the elongation zone, and intermediate pH (7–7.3) in the meristematic zone (133). Using ratiometric pHluorin researchers reported pH gradients and pH oscillations in tobacco pollen tubes (32). Cytoplasmic pH oscillations in root hairs were also observed by using the pH-sensitive GFP (H148D) (128). Ratiometric pHluorin has also been used to estimate apoplastic pH (62), and a whole palette of targeted ratiometric pHluorin variants has been used recently to map the pH in various subcellular compartments and organelles (120, 176). Reported data indicate a pH gradient within the endomembrane system (120, 176).

Compared with phGFP, Pt-GFP has been successfully established in *Arabidopsis* to monitor anoxia-induced acidification in roots (169) and to investigate whether changes in [CO_2] affect guard cell pH (206). A third pH biosensor, apo-pHusion, targeted to the apoplast enabled monitoring of auxin-induced apoplastic alkalinization in the root elongation zone (65). In hypocotyls, use of apo-pHusion indicates auxin- and gravity-induced apoplastic acidifications that depend on the canonical TIR/AFB-AUX/IAA auxin signaling pathway (58). pHusion was also used to determine steady-state pH in the *trans*-Golgi network/early endosome (TGN/EE) and in *trans*-Golgi cisternae (117). Data indicate that reduced V-ATPase activity in the *det3* mutant (171) affects the

steady-state pH in the TGN/EE but not in *trans*-Golgi cisternae (117). Note that steady-state pH values in the TGN/EE (pH 5.6) and *trans*-Golgi cisternae (pH 6.3) determined with pHusion (117) were not consistent with values determined with ratiometric pHluorin (TGN pH 6.3 and 6.1, *trans*-Golgi cisternae pH 6.9) (120, 176). These variations may result from different calibration protocols. However, owing to its more acidic pK_a, pHusion more reliably reports the pH in acidic environments (65).

PRIMARY METABOLITES

Although widely distributed, the concentration of central metabolites can vary across spatial and temporal scales, depending on subcellular compartment, cell type, developmental stage, and physiological condition. In many cases, little is known about the concentration of a given metabolite in plant cell compartments or about how metabolite concentrations are regulated at the cellular or subcellular level. The use of biosensors can help to fill these knowledge gaps, and early studies using metabolite biosensors have proven particularly valuable in both the discovery and characterization of metabolite transport activities. A seminal study that made use of a suite of four glucose biosensors (FLIPglu-Δ13) with affinities ranging from $K_d = 170$ nM to $K_d = 3.2$ mM first indicated that cytoplasmic glucose concentrations in leaf epidermal cells are lower than those in root cells (50). FLIPglu-Δ13 glucose biosensors with $K_d = 2$ μM and 170 nM were responsive to pulsed treatments with exogenous glucose in root cells, but nonresponsive in leaf cells owing to apparent saturation prior to treatment (50). The surprisingly large range of biosensors responsive to glucose in vivo indicates that glucose levels are not under tight homeostatic control in relation to exogenous glucose levels. Subsequent improvements in root-imaging modalities (**Figure 3**) that couple tighter temporal control over the liquid perfusion environment have resulted in better quantitation of root responses to treatments with exogenous sugars [e.g., glucose and sucrose (36, 37) and glucose and galactose (70)]. FLIPglu-Δ13 glucose biosensors that have minimal response to sucrose in vitro respond to sucrose perfusion with 60–95% of their response to equimolar glucose treatments when expressed in root cells, demonstrating that sucrolysis is rapid under the conditions tested (37). Long-term perfusion time-course measurements of root growth and the FLII12Pglu-700μ∂6 biosensor that detects glucose and galactose in vitro indicate that glucose stabilizes root growth in darkness shortly after the start of perfusion but galactose stops root growth completely after 5 h of perfusion (70).

Such perfusion experiments can also be used to probe transport properties, for example, the accumulation of exogenous glucose as measured with FLIPglu-600μΔ13 and exogenous sucrose as measured with FLIPsuc-90μΔ1 (**Figure 4**) (37). Results indicate that the sugar transporters known at the time, which depend on the proton gradient, were not responsible for the observed transport properties. A subsequent screen in HEK293T cells expressing *Arabidopsis* proteins along with a FRET biosensor for glucose led to the discovery of the SWEET family of sugar uniporters that contribute to sugar export in vivo (39). A similar progression for studies of amino acid transport involved characterization of partly protonophore-insensitive glutamine transport in *Arabidopsis* roots by using a glutamine biosensor (207) and resulted in the discovery of UMAMIT amino acid uniporters that contribute to amino acid export in vivo (26, 106, 135). Although the majority of studies have focused on imaging in *Arabidopsis*, expression of glucose biosensors in rice has revealed rapid and reversible glucose increases in vivo in response to several signals and stresses beyond glucose. These responses fall in the detection range of the FLIPglu-2 μΔ13 biosensor with $K_d = 2$ μM (212).

Recently, an ATP sensor (ATeam) (99) that was originally characterized for use in mammalian cells was deployed in *Arabidopsis*. ATeam1.03-nD/nA reports $MgATP^{2-}$ and was targeted to the

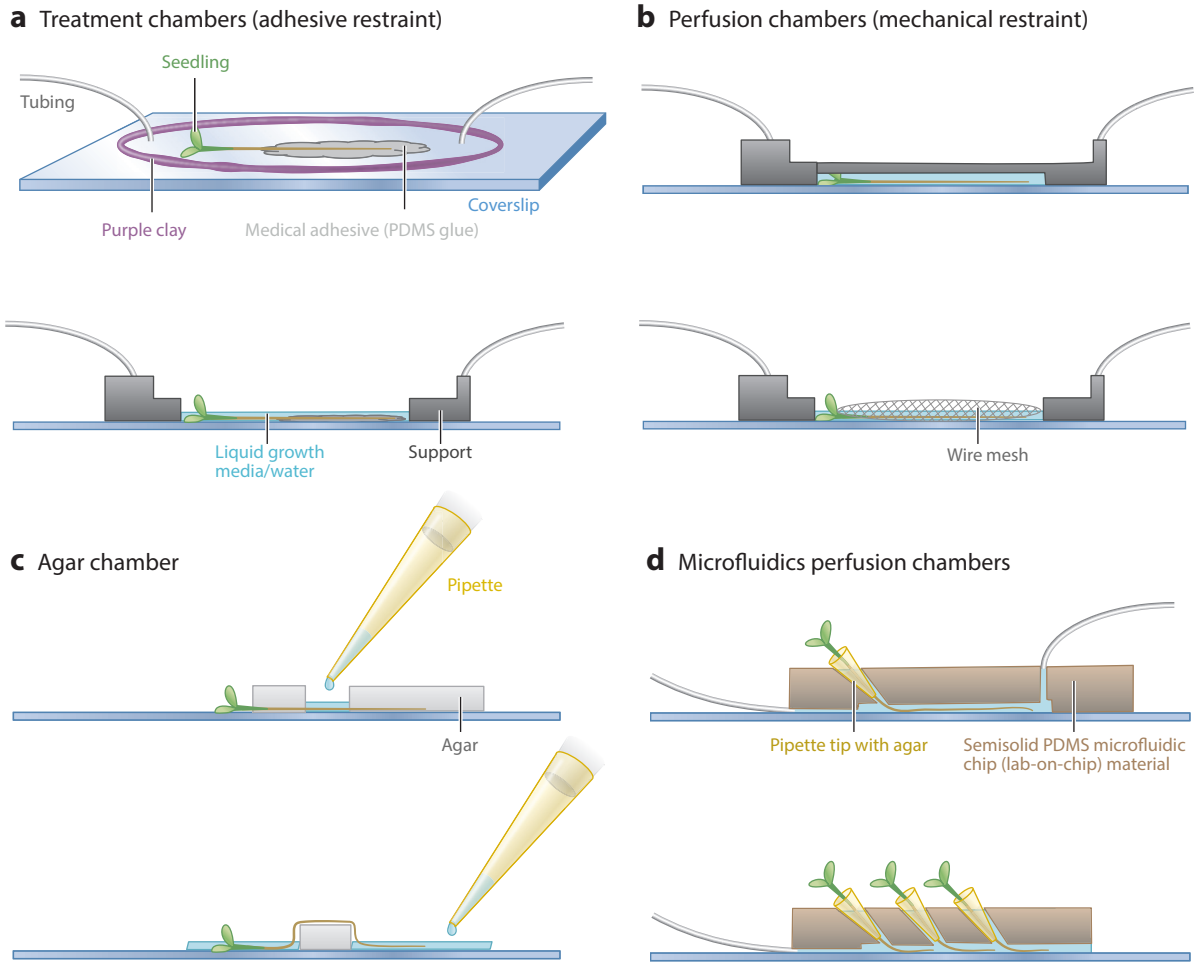

Figure 3

Schematic illustrations to show example imaging modalities to image plants expressing biosensors. (*a*) Chambers using adhesive restraint to monitor the response of plants to short-term treatments (36). (*b*) Perfusion-based chambers using mechanical restraint to monitor plant responses to various treatments using custom-built chambers (102, 168), Ibidi slides (38), or SecureSeal™ (161). (*c*) Agar-based approach to monitor changes in biosensor ratio (131, 160, 197). (*d*) Microfluidics-based perfusion chamber to monitor plant root responses (70, 182). Abbreviation: PDMS, polydimethylsiloxane.

cytosol as well as to ATP-producing organelles (i.e., the chloroplast stroma and the mitochondrial matrix) to reveal spatiotemporal patterns of $MgATP^{2-}$ during normal development as well as during energy stress induced by hypoxia (47). In addition to characterizing $MgATP^{2-}$ steady-state patterning, substantial plasticity in $MgATP^{2-}$ was also revealed (47).

Abscisic acid concentration and uptake sensor (ABACUS): a FRET biosensor for abscisic acid detection

HORMONES

Two FRET-based biosensors for the phytohormone ABA have been developed that report on ABA dynamics in response to exogenous ABA or challenge with stress conditions (92, 197). ABACUS1 (abscisic acid concentration and uptake sensor) was engineered by linking an ABA sensory module (PYL1 fused to a highly truncated ABA interaction domain of ABI1) to edCerulean as FRET donor

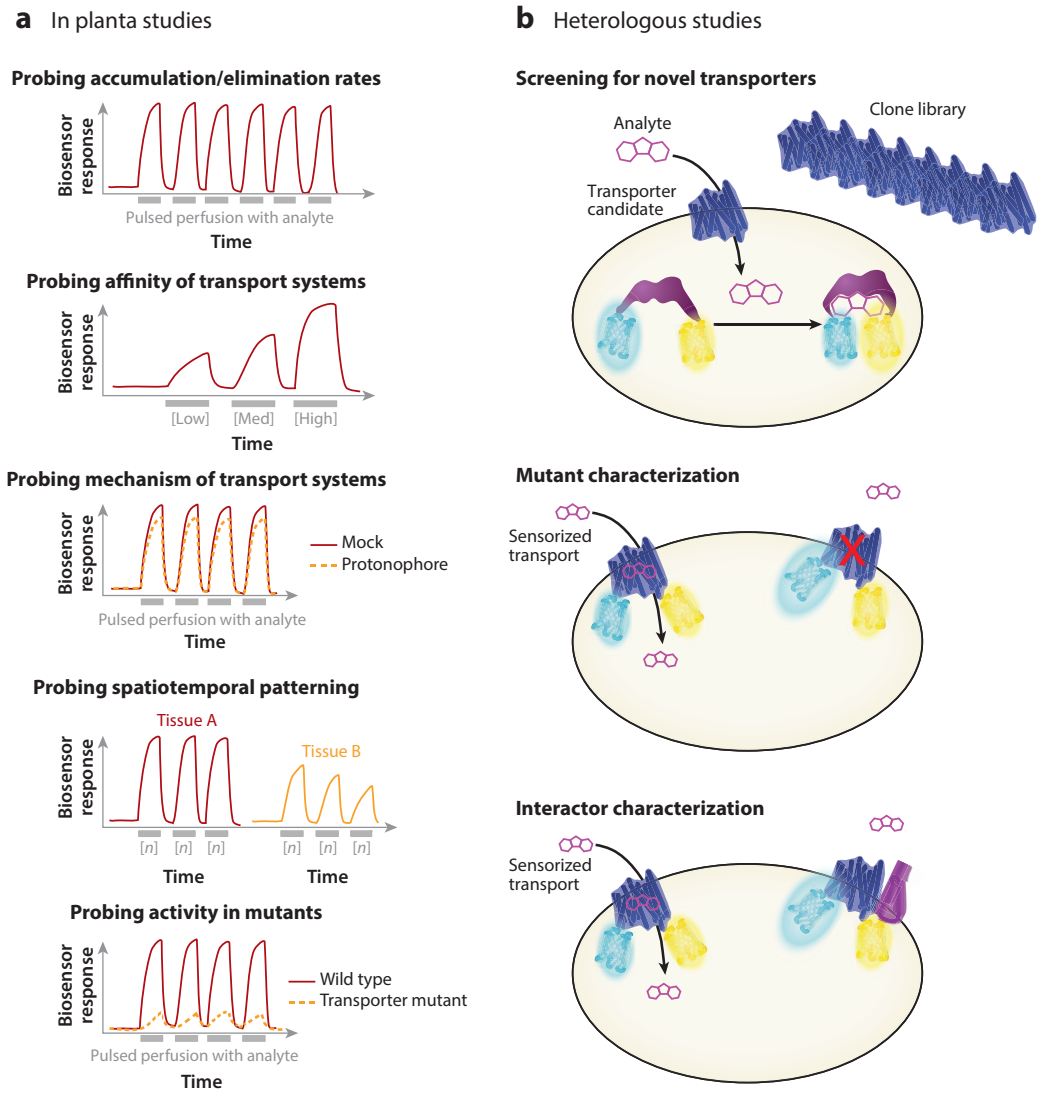

Figure 4

Biosensors for studying transport. (*a*) Genetically encoded biosensors have been used in planta to monitor accumulation and elimination rates during and following pulsed application of exogenous analytes (50). This approach allows for the interrogation of transport activities in vivo and can be applied to indirectly probe affinity (92), mechanisms (37), and spatiotemporal patterning (160) of transport activities. Such analyses can also reveal quantitative molecular phenotypes in mutant lines expressing biosensors (134). (*b*) Biosensors have been used in heterologous systems to screen for novel plant transporters [e.g., SWEET1 (39)] and, through the use of sensorized transporters, to rapidly interrogate the effects of mutations and protein interactions on the activity of plant transporters [e.g., NRT1.1/CHL1/NPF6.3 (81)].

and edCitrine as FRET acceptor (92). The ABACUS1 biosensor was used to detect reversible and dose-dependent ABA accumulation following pulsed ABA treatments in roots growing in RootChip16, showing that the ABA elimination rate is cell specific and accelerated by ABA (92). A similar but distinct ABA biosensor, ABAleon2.1, was engineered by fusing an ABA sensory module (PYR1 linked to catalytic domain of the ABI1) to mTurquoise as FRET donor and cpVenus173 as

ABAleon: a FRET biosensor for abscisic acid detection

FRET acceptor. ABAleon2.1 reported on endogenous ABA concentrations in response to abiotic stresses and was used to track the long-distance translocation of ABA among root, hypocotyl, and shoot tissues in response to exogenous application of ABA (197).

Gibberellin perception sensor (GPS): a FRET biosensor for detecting gibberellin

A recent FRET-based biosensor, gibberellin perception sensor 1 (GPS1), detects GA and was engineered by fusing a GA sensory module (AtGID1C GA receptor linked to the DELLA domain of AtGAI) with edCerulean as FRET donor and edAphrodite as FRET acceptor (160). GPS1 responds to nanomolar concentrations of bioactive GAs (e.g., $K_d = 24$ nM for GA_4) and exhibits slow apparent reversibility in vitro (160). Thus, GPS1 expressed in vivo can report increases in GA but does not report on GA depletion. Expression of GPS1 from a p16 promoter (172), which circumvents silencing observed previously (37, 50, 92), permits detection of a gradient of GA in dark-grown hypocotyls of wild-type and light-signaling mutants (160). GPS1 reports higher GA levels in larger cells of the dark-grown hypocotyl as compared with smaller cells near the apical hook, and apparent GA accumulation in the dark is reduced in a phytochrome-interacting factor quadruple mutant (160). GPS1 also reports an endogenous GA gradient in primary root tips, which is mirrored by an accumulation gradient of exogenous GA_4 (160). As such, GA patterning could be achieved in roots independently of patterns of GA biosynthesis.

NUTRIENTS

Inorganic Phosphate

Plants acquire and assimilate phosphorous in the form of inorganic phosphate (P_i), which is required for important cellular processes such as energy transfer reactions, signal transduction, and enzyme activities. cpFLIPPi is a second-generation FRET-based biosensor that detects P_i and consists of a cyanobacterial P_i-binding protein fused between eCFP as FRET donor and cpVenus as FRET acceptor. cpFLIPPi was recently developed and used in planta (134) to detect changes in cytoplasmic P_i concentrations in root epidermal cells in response to P_i starvation and replenishment. In addition, a plastid-targeted version of the cpFLIPPi sensor was used to assess the role of plastidic P_i transporter PHT4;2 in P_i transport (134).

Zinc

Researchers have developed high-affinity FRET-based Zn^{2+} sensors (e.g., eCALWY-1) that contain two metal-binding domains, ATOX1 and WD4, linked via a flexible linker and flanked by Cerulean as FRET donor and Citrine as FRET acceptor (195). Binding of Zn^{2+} between the two metal-binding domains causes a decrease in energy transfer that reveals Zn^{2+} concentrations. Using eCALWY-1 and modified versions in *Arabidopsis* root cells, Lanquar et al. (107) reported on cytoplasmic-free Zn^{2+} concentrations in roots supplied with varied exogenous Zn^{2+} concentrations using the RootChip (70). Experiments combining a FRET-based biosensor with the perfusion control afforded by the RootChip indicate the involvement of low- and high-affinity uptake systems as well as release of internal stores of Zn^{2+} governing Zn^{2+} homeostasis in living cells (107).

Nitrate and Ammonium Transport

Transporters for ammonium and nitrate ions act as dual-function transporter/receptors (transceptors) (10, 100, 112, 196), but the activity status of a specific transporter is difficult to assess within a living plant. De Michele et al. (48) created a transport-activity biosensor by inserting a circularly permutated GFP (mcpGFP) into the cytoplasmic loop of the *Arabidopsis* ammonium transporter

AMT1;3. This intensiometric approach is based on tracking mcpGFP fluorescence changes that result from conformational changes in AMT1;3 that occur during transport. Yeast cells expressing AMT1;3-mcpGFP biosensors (AmTracs) show concentration-dependent fluorescence intensity changes in response to ammonium chloride treatments that correlate with the transport activity of AMT1;3. The same approach was used to create two more ammonium transport activity-state biosensors. These chimeric AmTrac1;2 and MepTrac biosensors maintain transporter activity in yeast cells and exhibit intensiometric fluorescence responses to ammonium treatments (48) (**Figure 4*b***). Ast et al. (12) characterized the photophysical properties of different AmTrac biosensors and replaced key amino acid residues in the mcpGFP of AmTrac to construct a set of ratiometric dual-emission AmTrac biosensors termed deAmTracs.

Ho & Frommer (81) sandwiched the *Arabidopsis* nitrate transceptor CHL1 between mCerulean and Aphrodite and exploited conformational rearrangements during the transporter cycle that quenched fluorescence of the mCerulean moiety. The chimera NiTrac1 was used to report on the movement of nitrate through yeast cell membranes. Measurements of the NiTrac1 response in yeast cells demonstrate nitrate-induced quenching that is reversible in nature after nitrate removal (81). Researchers also created similar constructs for the oligopeptide transporters PTR1, PTR2, PTR4, and PTR5 from *Arabidopsis* and found they exhibit peptide-specific quenching. Furthermore, NiTrac1 expressed in yeast was used to facilitate testing the effects of CHL1 mutations and protein-protein interactions on nitrate transport (81) (**Figure 4*b***). Taken together, these investigations utilizing activity-state sensors in yeast cells have significantly increased our understanding of transporter behavior. Yet application of these biosensors to in planta characterizations awaits further experimentation.

MULTICOLOR AND MULTIPARAMETER ANALYSES USING FLUORESCENT REPORTERS

Multicolor and multiparameter analyses rely on the principle that two or more genetically encoded fluorescent biosensors with distinct fluorescence properties are coexpressed in the same plant and tissue and are imaged simultaneously at the microscope. Multicolor approaches can monitor one analyte in multiple compartments or cell types while using multiple biosensors with distinct localization and fluorescence properties. Multiparameter analyses monitor multiple analytes while using fluorescent biosensors with distinct analyte-binding and fluorescent properties. Multicolor fluorescent biosensors were first developed for calcium (3, 211; for a summary, also see 154) and are now also available for ROS and redox (27) and pH measurements (22). Most fluorescent biosensors are cyan/yellow FRET based or green emitting (**https://codex.dpb.carnegiescience.edu/db/biosensor**). Therefore, key for the achievement of multicolor/multiparameter analyses was the development of red-emitting fluorescent biosensors.

Multicolor calcium imaging has been reported in which the cytoplasm- and nucleus-localized red-emitting R-GECO1 was coexpressed with cytoplasmic cyan/yellow FRET-based YC3.6 (93). Although this study mainly compared the in vivo properties of both GECIs, it demonstrated that the signal changes of R-GECO1 are more than tenfold higher than those of YC3.6 in response to ATP and hyperpolarization buffer (93). Through expression of R-GECO1 in pollen tubes and YC3.6 in synergids it was for the first time possible to spatially resolve calcium signals during double fertilization (144) (for details see the section titled Calcium Imaging in Pollen Tubes and During Fertilization), demonstrating the huge potential of multicolor imaging approaches in plants.

Multiparameter analyses using the cyan/yellow FRET-based biosensor ABAleon2.1 (197) and R-GECO1 (211) were recently employed to simultaneously image ABA and calcium, respectively (199). Hormone response analyses in young roots indicate that ABA is rapidly taken up but does

not trigger rapid calcium signals. By contrast, auxin induces calcium signals but does not trigger rapid ABA concentration changes (199). Through the use of R-GECO1 and other red-emitting biosensors for calcium, ROS and redox, or pH (see above), the dynamic changes of at least two of these molecules may now be resolved and correlated at the same time. In addition, red-emitting biosensors may be combined with any cyan/yellow FRET-based and blue- or green-emitting biosensors. Finally, direct cyan/yellow FRET-based readouts may also be combined with indirect red-emitting transcriptional readouts.

SUMMARY AND OUTLOOK

Molecules or molecular events whose variation in concentration or activity is physiologically relevant are prime targets for biosensing approaches. For multiorganellar and multicellular eukaryotes, the spatiotemporal information obtainable with a biosensor is particularly important. This is true for understanding both the regulatory and biochemical activities that influence the spatiotemporal patterns of a molecule or molecular event of interest and the physiological consequences of such patterns. Starting from initial biosensor engineering, in vivo analysis of several analytes has now progressed sufficiently through optimization of biosensor performance, expression in planta, and imaging modalities such that novel spatiotemporal patterns are being discovered and characterized in a variety of biological systems. Most analytes still lack biosensors, however, and most extant biosensors have yet to be deployed in plants. Thus, we have only begun to tap the potential of biosensor-based analysis. Fortunately, new biosensors based on high-specificity sensory proteins, e.g., for MAP kinase signaling (P. Krysan, personal communication), continue to be engineered, and there is further promise for a more generalized approach based on incorporating RNA aptamers or antibodies selected for requisite specificity into genetically encoded biosensors (145). Furthermore, with little to no reengineering, direct biosensors developed for use in other organisms are often functional in plants (47, 107). As a result, the barrier to the first application in plants of an extant biosensor is often low.

SUMMARY POINTS

1. Biosensors present an opportunity to monitor real-time dynamics of molecules or molecular events in various cell and tissue types.
2. Biosensor measurements can integrate with cell biological data, high-resolution transcriptional profiling, and computational modeling to build an integrated picture of biological processes.
3. Biosensors are valuable tools to monitor analyte distributions (e.g., hormone gradients) in the context of multicellular tissues.
4. Ratiometric biosensors (e.g., FRET-based biosensors) can help avoid artefacts associated with loss or gain of signal stemming from changes in biosensor expression or imaging multiple tissue layers.
5. For a given analyte, development of several biosensors with varying affinities is important to better understand endogenous cellular dynamics in response to developmental and environmental cues.
6. The evolution of GECIs over the past 20 years led to the discovery of general principles for biosensor designs that can now be exploited for the generation of direct biosensors for other small molecules.

7. In multicolor and multiparameter approaches, the coexpression of multiple biosensors within the same tissues will provide future opportunities to correlate biosensor outputs with one another.
8. The continued development of imaging modalities will further enable quantitative analysis of biosensors in additional tissue, environmental, and organismal contexts.

DISCLOSURE STATEMENT

The authors are not aware of any affiliations, memberships, funding, or financial holdings that might be perceived as affecting the objectivity of this review.

ACKNOWLEDGMENTS

A.W. and A.M.J. were supported by a Gatsby Research Fellowship awarded to A.M.J. R.W. was supported by the Deutsche Forschungsgemeinschaft (WA 3768/1–1).

LITERATURE CITED

1. Achard P, Cheng H, De Grauwe L, Decat J, Schoutteten H, et al. 2006. Integration of plant responses to environmentally activated phytohormonal signals. *Science* 311:91–94
2. Achard P, Liao L, Jiang C, Desnos T, Bartlett J, et al. 2007. DELLAs contribute to plant photomorphogenesis. *Plant Physiol.* 143:1163–72
3. Akerboom J, Carreras Calderon N, Tian L, Wabnig S, Prigge M, et al. 2013. Genetically encoded calcium indicators for multi-color neural activity imaging and combination with optogenetics. *Front. Mol. Neurosci.* 6:2
4. Akerboom J, Chen TW, Wardill TJ, Tian L, Marvin JS, et al. 2012. Optimization of a GCaMP calcium indicator for neural activity imaging. *J. Neurosci.* 32:13819–40
5. Alford SC, Abdelfattah AS, Ding Y, Campbell RE. 2012. A fluorogenic red fluorescent protein heterodimer. *Chem. Biol.* 19:353–60
6. Alford SC, Wu J, Zhao Y, Campbell RE, Knopfel T. 2013. Optogenetic reporters. *Biol. Cell* 105:14–29
7. Allen GJ, Chu SP, Harrington CL, Schumacher K, Hoffmann T, et al. 2001. A defined range of guard cell calcium oscillation parameters encodes stomatal movements. *Nature* 411:1053–57
8. Allen GJ, Chu SP, Schumacher K, Shimazaki CT, Vafeados D, et al. 2000. Alteration of stimulus-specific guard cell calcium oscillations and stomatal closing in *Arabidopsis det3* mutant. *Science* 289:2338–42
9. Allen GJ, Kwak JM, Chu SP, Llopis J, Tsien RY, et al. 1999. Cameleon calcium indicator reports cytoplasmic calcium dynamics in *Arabidopsis* guard cells. *Plant J.* 19:735–47
10. Andrade SL, Einsle O. 2007. The Amt/Mep/Rh family of ammonium transport proteins. *Mol. Membr. Biol.* 24:357–65
11. **Arosio D, Ricci F, Marchetti L, Gualdani R, Albertazzi L, Beltram F. 2010. Simultaneous intracellular chloride and pH measurements using a GFP-based sensor. *Nat. Methods* 7:516–18**
12. Ast C, De Michele R, Kumke MU, Frommer WB. 2015. Single-fluorophore membrane transport activity sensors with dual-emission read-out. *eLife* 4:e07113
13. Ast C, Foret J, Oltrogge LM, De Michele R, Kleist TJ, et al. 2017. Ratiometric Matryoshka biosensors from a nested cassette of green- and orange-emitting fluorescent proteins. *Nat. Commun.* 8:431
14. Baird GS, Zacharias DA, Tsien RY. 1999. Circular permutation and receptor insertion within green fluorescent proteins. *PNAS* 96:11241–46
15. Band LR, Wells DM, Fozard JA, Ghetiu T, French AP, et al. 2014. Systems analysis of auxin transport in the *Arabidopsis* root apex. *Plant Cell* 26:862–75
16. Band LR, Wells DM, Larrieu A, Sun J, Middleton AM, et al. 2012. Root gravitropism is regulated by a transient lateral auxin gradient controlled by a tipping-point mechanism. *PNAS* 109:4668–73

11. Describes the design of a dual-excitation and triple-emission biosensor that can monitor chloride and pH changes at the same time.

17. Barbez E, Dunser K, Gaidora A, Lendl T, Busch W. 2017. Auxin steers root cell expansion via apoplastic pH regulation in *Arabidopsis thaliana*. *PNAS* 114:E4884–93
18. Bassil E, Blumwald E. 2014. The ins and outs of intracellular ion homeostasis: NHX-type cation/H^+ transporters. *Curr. Opin. Plant Biol.* 22:1–6
19. Behera S, Long Y, Schmitz-Thom I, Wang XP, Zhang C, et al. 2017. Two spatially and temporally distinct Ca^{2+} signals convey *Arabidopsis thaliana* responses to K^+ deficiency. *New Phytol*. 213:739–50
20. Behera S, Wang N, Zhang C, Schmitz-Thom I, Strohkamp S, et al. 2015. Analyses of Ca^{2+} dynamics using a ubiquitin-10 promoter-driven Yellow Cameleon 3.6 indicator reveal reliable transgene expression and differences in cytoplasmic Ca^{2+} responses in Arabidopsis and rice (*Oryza sativa*) roots. *New Phytol*. 206:751–60
21. Belousov VV, Fradkov AF, Lukyanov KA, Staroverov DB, Shakhbazov KS, et al. 2006. Genetically encoded fluorescent indicator for intracellular hydrogen peroxide. *Nat. Methods* 3:281–86
22. Bencina M. 2013. Illumination of the spatial order of intracellular pH by genetically encoded pH-sensitive sensors. *Sensors* 13:16736–58
23. Bencivenga S, Simonini S, Benkova E, Colombo L. 2012. The transcription factors BEL1 and SPL are required for cytokinin and auxin signaling during ovule development in *Arabidopsis*. *Plant Cell* 24:2886–97
24. Benkova E, Michniewicz M, Sauer M, Teichmann T, Seifertova D, et al. 2003. Local, efflux-dependent auxin gradients as a common module for plant organ formation. *Cell* 115:591–602
25. Berlin S, Carroll EC, Newman ZL, Okada HO, Quinn CM, et al. 2015. Photoactivatable genetically encoded calcium indicators for targeted neuronal imaging. *Nat. Methods* 12:852–58
26. Besnard J, Pratelli R, Zhao C, Sonawala U, Collakova E, et al. 2016. UMAMIT14 is an amino acid exporter involved in phloem unloading in Arabidopsis roots. *J. Exp. Bot.* 67:6385–97
27. Bilan DS, Belousov VV. 2017. New tools for redox biology: from imaging to manipulation. *Free Radic. Biol. Med.* 109:167–88
28. Bonza MC, Loro G, Behera S, Wong A, Kudla J, Costa A. 2013. Analyses of Ca^{2+} accumulation and dynamics in the endoplasmic reticulum of Arabidopsis root cells using a genetically encoded Cameleon sensor. *Plant Physiol*. 163:1230–41
29. Bratt A, Rosenwasser S, Meyer A, Fluhr R. 2016. Organelle redox autonomy during environmental stress. *Plant Cell Environ*. 39:1909–19
30. Brunoud G, Wells DM, Oliva M, Larrieu A, Mirabet V, et al. 2012. A novel sensor to map auxin response and distribution at high spatio-temporal resolution. *Nature* 482:103–6
31. Capoen W, Sun J, Wysham D, Otegui MS, Venkateshwaran M, et al. 2011. Nuclear membranes control symbiotic calcium signaling of legumes. *PNAS* 108:14348–53
32. Certal AC, Almeida RB, Carvalho LM, Wong E, Moreno N, et al. 2008. Exclusion of a proton ATPase from the apical membrane is associated with cell polarity and tip growth in *Nicotiana tabacum* pollen tubes. *Plant Cell* 20:614–34
33. Chaiwanon J, Wang ZY. 2015. Spatiotemporal brassinosteroid signaling and antagonism with auxin pattern stem cell dynamics in *Arabidopsis* roots. *Curr. Biol.* 25:1031–42
34. Chapleau RR, Blomberg R, Ford PC, Sagermann M. 2008. Design of a highly specific and noninvasive biosensor suitable for real-time in vivo imaging of mercury (II) uptake. *Protein Sci*. 17:614–22
35. Charpentier M, Sun J, Vaz Martins T, Radhakrishnan GV, Findlay K, et al. 2016. Nuclear-localized cyclic nucleotide-gated channels mediate symbiotic calcium oscillations. *Science* 352:1102–5
36. Chaudhuri B, Hormann F, Frommer WB. 2011. Dynamic imaging of glucose flux impedance using FRET sensors in wild-type *Arabidopsis* plants. *J. Exp. Bot.* 62:2411–17
37. Chaudhuri B, Hormann F, Lalonde S, Brady SM, Orlando DA, et al. 2008. Protonophore- and pH-insensitive glucose and sucrose accumulation detected by FRET nanosensors in Arabidopsis root tips. *Plant J.* 56:948–62
38. Chebli Y, Pujol L, Shojaeifard A, Brouwer I, van Loon JJ, Geitmann A. 2013. Cell wall assembly and intracellular trafficking in plant cells are directly affected by changes in the magnitude of gravitational acceleration. *PLOS ONE* 8:e58246
39. Chen LQ, Hou BH, Lalonde S, Takanaga H, Hartung ML, et al. 2010. Sugar transporters for intercellular exchange and nutrition of pathogens. *Nature* 468:527–32

40. Chen TW, Wardill TJ, Sun Y, Pulver SR, Renninger SL, et al. 2013. Ultrasensitive fluorescent proteins for imaging neuronal activity. *Nature* 499:295–300
41. Cho J-H, Swanson CJ, Chen J, Li A, Lippert LG, et al. 2017. The GCaMP-R family of genetically encoded ratiometric calcium indicators. *ACS Chem. Biol.* 12:1066–74
42. Choi WG, Hilleary R, Swanson SJ, Kim SH, Gilroy S. 2016. Rapid, long-distance electrical and calcium signaling in plants. *Annu. Rev. Plant Biol.* 67:287–307
43. Choi WG, Swanson SJ, Gilroy S. 2012. High-resolution imaging of Ca^{2+}, redox status, ROS and pH using GFP biosensors. *Plant J.* 70:118–28
44. Choi WG, Toyota M, Kim SH, Hilleary R, Gilroy S. 2014. Salt stress-induced Ca^{2+} waves are associated with rapid, long-distance root-to-shoot signaling in plants. *PNAS* 111:6497–502
45. Costa A, Drago I, Behera S, Zottini M, Pizzo P, et al. 2010. H_2O_2 in plant peroxisomes: an in vivo analysis uncovers a Ca^{2+}-dependent scavenging system. *Plant J.* 62:760–72
46. Costa A, Kudla J. 2015. Colorful insights: advances in imaging drive novel breakthroughs in Ca^{2+} signaling. *Mol. Plant* 8:352–55
47. De Col V, Fuchs P, Nietzel T, Elsasser M, Voon CP, et al. 2017. ATP sensing in living plant cells reveals tissue gradients and stress dynamics of energy physiology. *eLife* 6:e26670
48. De Michele R, Ast C, Loque D, Ho CH, Andrade S, et al. 2013. Fluorescent sensors reporting the activity of ammonium transceptors in live cells. *eLife* 2:e00800
49. Denninger P, Bleckmann A, Lausser A, Vogler F, Ott T, et al. 2014. Male-female communication triggers calcium signatures during fertilization in *Arabidopsis*. *Nat. Commun.* 5:4645
50. **Deuschle K, Chaudhuri B, Okumoto S, Lager I, Lalonde S, Frommer WB. 2006. Rapid metabolism of glucose detected with FRET glucose nanosensors in epidermal cells and intact roots of *Arabidopsis* RNA-silencing mutants. *Plant Cell* 18:2314–25**
51. Dill A, Jung HS, Sun TP. 2001. The DELLA motif is essential for gibberellin-induced degradation of RGA. *PNAS* 98:14162–67
52. **Ding Y, Li J, Enterina JR, Shen Y, Zhang I, et al. 2015. Ratiometric biosensors based on dimerization-dependent fluorescent protein exchange. *Nat. Methods* 12:195–98**
53. Dodd AN, Kudla J, Sanders D. 2010. The language of calcium signaling. *Annu. Rev. Plant Biol.* 61:593–620
54. Dohmann EM, Nill C, Schwechheimer C. 2010. DELLA proteins restrain germination and elongation growth in *Arabidopsis thaliana* COP9 signalosome mutants. *Eur. J. Cell Biol.* 89:163–68
55. Dong TX, Othy S, Jairaman A, Skupsky J, Zavala A, et al. 2017. T cell calcium dynamics visualized in a ratiometric tdTomato-GCaMP6f transgenic reporter mouse. *eLife* 6:e32417
56. Duan L, Dietrich D, Ng CH, Chan PM, Bhalerao R, et al. 2013. Endodermal ABA signaling promotes lateral root quiescence during salt stress in *Arabidopsis* seedlings. *Plant Cell* 25:324–41
57. Evans MJ, Choi WG, Gilroy S, Morris RJ. 2016. A ROS-assisted calcium wave dependent on the AtRBOHD and TPC1 cation channel propagates the systemic response to salt stress. *Plant Physiol.* 171:1771–84
58. Fendrych M, Leung J, Friml J. 2016. TIR1/AFB-Aux/IAA auxin perception mediates rapid cell wall acidification and growth of Arabidopsis hypocotyls. *eLife* 5:e19048
59. Figueiredo DD, Batista RA, Roszak PJ, Hennig L, Kohler C. 2016. Auxin production in the endosperm drives seed coat development in *Arabidopsis*. *eLife* 5:e20542
60. Fosque BF, Sun Y, Dana H, Yang CT, Ohyama T, et al. 2015. Labeling of active neural circuits in vivo with designed calcium integrators. *Science* 347:755–60
61. Galietta LJ, Haggie PM, Verkman AS. 2001. Green fluorescent protein-based halide indicators with improved chloride and iodide affinities. *FEBS Lett.* 499:220–24
62. Gao D, Knight MR, Trewavas AJ, Sattelmacher B, Plieth C. 2004. Self-reporting Arabidopsis expressing pH and [Ca^{2+}] indicators unveil ion dynamics in the cytoplasm and in the apoplast under abiotic stress. *Plant Physiol.* 134:898–908
63. Gao QF, Gu LL, Wang HQ, Fei CF, Fang X, et al. 2016. Cyclic nucleotide-gated channel 18 is an essential Ca^{2+} channel in pollen tube tips for pollen tube guidance to ovules in *Arabidopsis*. *PNAS* 113:3096–101

50. Seminal work demonstrating glucose measurements in multiple tissues as well as the utility of optimization and diversification of biosensor properties.

52. Introduces a new concept for biosensor design using dimerization-dependent fluorescent proteins.

64. Garcia-Plazaola JI, Fernandez-Marin B, Duke SO, Hernandez A, Lopez-Arbeloa F, Becerril JM. 2015. Autofluorescence: biological functions and technical applications. *Plant Sci*. 236:136–45
65. Gjetting KS, Ytting CK, Schulz A, Fuglsang AT. 2012. Live imaging of intra- and extracellular pH in plants using pHusion, a novel genetically encoded biosensor. *J. Exp. Bot.* 63:3207–18
66. Gjetting SK, Schulz A, Fuglsang AT. 2013. Perspectives for using genetically encoded fluorescent biosensors in plants. *Front. Plant Sci.* 4:234
67. Gordon SP, Chickarmane VS, Ohno C, Meyerowitz EM. 2009. Multiple feedback loops through cytokinin signaling control stem cell number within the *Arabidopsis* shoot meristem. *PNAS* 106:16529–34
68. Gould SJ, Subramani S. 1988. Firefly luciferase as a tool in molecular and cell biology. *Anal. Biochem.* 175:5–13
69. Griesbeck O, Baird GS, Campbell RE, Zacharias DA, Tsien RY. 2001. Reducing the environmental sensitivity of yellow fluorescent protein: mechanism and applications. *J. Biol. Chem.* 276:29188–94
70. Grossmann G, Guo WJ, Ehrhardt DW, Frommer WB, Sit RV, et al. 2011. The RootChip: an integrated microfluidic chip for plant science. *Plant Cell* 23:4234–40
71. Gutermuth T, Lassig R, Portes MT, Maierhofer T, Romeis T, et al. 2013. Pollen tube growth regulation by free anions depends on the interaction between the anion channel SLAH3 and calcium-dependent protein kinases CPK2 and CPK20. *Plant Cell* 25:4525–43
72. Hamamura Y, Nishimaki M, Takeuchi H, Geitmann A, Kurihara D, Higashiyama T. 2014. Live imaging of calcium spikes during double fertilization in *Arabidopsis. Nat. Commun*. 5:4722
73. Hamilton DW, Hills A, Kohler B, Blatt MR. 2000. Ca^{2+} channels at the plasma membrane of stomatal guard cells are activated by hyperpolarization and abscisic acid. *PNAS* 97:4967–72
74. Han S, Tang R, Anderson LK, Woerner TE, Pei ZM. 2003. A cell surface receptor mediates extracellular Ca^{2+} sensing in guard cells. *Nature* 425:196–200
75. Hanson GT, Aggeler R, Oglesbee D, Cannon M, Capaldi RA, et al. 2004. Investigating mitochondrial redox potential with redox-sensitive green fluorescent protein indicators. *J. Biol. Chem.* 279:13044–53
76. Hanson GT, McAnaney TB, Park ES, Rendell ME, Yarbrough DK, et al. 2002. Green fluorescent protein variants as ratiometric dual emission pH sensors. 1. Structural characterization and preliminary application. *Biochemistry* 41:15477–88
77. Haruta M, Monshausen G, Gilroy S, Sussman MR. 2008. A cytoplasmic Ca^{2+} functional assay for identifying and purifying endogenous cell signaling peptides in *Arabidopsis* seedlings: identification of AtRALF1 peptide. *Biochemistry* 47:6311–21
78. Heim N, Griesbeck O. 2004. Genetically encoded indicators of cellular calcium dynamics based on troponin C and green fluorescent protein. *J. Biol. Chem.* 279:14280–86
79. Heisler MG, Ohno C, Das P, Sieber P, Reddy GV, et al. 2005. Patterns of auxin transport and gene expression during primordium development revealed by live imaging of the *Arabidopsis* inflorescence meristem. *Curr. Biol.* 15:1899–911
80. Hernandez-Barrera A, Velarde-Buendia A, Zepeda I, Sanchez F, Quinto C, et al. 2015. Hyper, a hydrogen peroxide sensor, indicates the sensitivity of the *Arabidopsis* root elongation zone to aluminum treatment. *Sensors* 15:855–67
81. Ho CH, Frommer WB. 2014. Fluorescent sensors for activity and regulation of the nitrate transceptor CHL1/NRT1.1 and oligopeptide transporters. *eLife* 3:e01917
82. Hoi H, Matsuda T, Nagai T, Campbell RE. 2013. Highlightable Ca^{2+} indicators for live cell imaging. *J. Am. Chem. Soc.* 135:46–49
83. Horikawa K, Yamada Y, Matsuda T, Kobayashi K, Hashimoto M, et al. 2010. Spontaneous network activity visualized by ultrasensitive Ca^{2+} indicators, yellow Cameleon-Nano. *Nat. Methods* 7:729–32
84. Hossain MA, Munemasa S, Uraji M, Nakamura Y, Mori IC, Murata Y. 2011. Involvement of endogenous abscisic acid in methyl jasmonate-induced stomatal closure in *Arabidopsis. Plant Physiol*. 156:430–38
85. Islam MM, Hossain MA, Jannat R, Munemasa S, Nakamura Y, et al. 2010. Cytosolic alkalization and cytosolic calcium oscillation in *Arabidopsis* guard cells response to ABA and MeJA. *Plant Cell Physiol*. 51:1721–30
86. Iwano M, Entani T, Shiba H, Kakita M, Nagai T, et al. 2009. Fine-tuning of the cytoplasmic Ca^{2+} concentration is essential for pollen tube growth. *Plant Physiol*. 150:1322–34

87. Iwano M, Ito K, Fujii S, Kakita M, Asano-Shimosato H, et al. 2015. Calcium signalling mediates self-incompatibility response in the Brassicaceae. *Nat. Plants* 1:15128
88. Iwano M, Ngo QA, Entani T, Shiba H, Nagai T, et al. 2012. Cytoplasmic Ca^{2+} changes dynamically during the interaction of the pollen tube with synergid cells. *Development* 139:4202–9
89. Iwano M, Shiba H, Miwa T, Che FS, Takayama S, et al. 2004. Ca^{2+} dynamics in a pollen grain and papilla cell during pollination of *Arabidopsis. Plant Physiol.* 136:3562–71
90. Jayaraman S, Haggie P, Wachter RM, Remington SJ, Verkman AS. 2000. Mechanism and cellular applications of a green fluorescent protein-based halide sensor. *J. Biol. Chem.* 275:6047–50
91. Jiang K, Schwarzer C, Lally E, Zhang S, Ruzin S, et al. 2006. Expression and characterization of a redox-sensing green fluorescent protein (reduction-oxidation-sensitive green fluorescent protein) in *Arabidopsis. Plant Physiol.* 141:397–403
92. Jones AM, Danielson JA, Manojkumar SN, Lanquar V, Grossmann G, Frommer WB. 2014. Abscisic acid dynamics in roots detected with genetically encoded FRET sensors. *eLife* 3:e01741
93. Keinath NF, Waadt R, Brugman R, Schroeder JI, Grossmann G, et al. 2015. Live cell imaging with R-GECO1 sheds light on flg22- and chitin-induced transient $[Ca^{2+}]$cyt patterns in *Arabidopsis. Mol. Plant* 8:1188–200
94. Khokon MA, Jahan MS, Rahman T, Hossain MA, Muroyama D, et al. 2011. Allyl isothiocyanate (AITC) induces stomatal closure in *Arabidopsis. Plant Cell Environ.* 34:1900–6
95. Klusener B, Young JJ, Murata Y, Allen GJ, Mori IC, et al. 2002. Convergence of calcium signaling pathways of pathogenic elicitors and abscisic acid in Arabidopsis guard cells. *Plant Physiol.* 130:2152–63
96. Kocsy G, Tari I, Vankova R, Zechmann B, Gulyas Z, et al. 2013. Redox control of plant growth and development. *Plant Sci.* 211:77–91
97. Konrad KR, Wudick MM, Feijo JA. 2011. Calcium regulation of tip growth: new genes for old mechanisms. *Curr. Opin. Plant Biol.* 14:721–30
98. Kosuta S, Hazledine S, Sun J, Miwa H, Morris RJ, et al. 2008. Differential and chaotic calcium signatures in the symbiosis signaling pathway of legumes. *PNAS* 105:9823–28
99. Kotera I, Iwasaki T, Imamura H, Noji H, Nagai T. 2010. Reversible dimerization of *Aequorea victoria* fluorescent proteins increases the dynamic range of FRET-based indicators. *ACS Chem. Biol.* 5:215–22
100. Kotur Z, Mackenzie N, Ramesh S, Tyerman SD, Kaiser BN, Glass AD. 2012. Nitrate transport capacity of the *Arabidopsis thaliana* NRT2 family members and their interactions with AtNAR2.1. *New Phytol.* 194:724–31
101. Krebs M, Held K, Binder A, Hashimoto K, Den Herder G, et al. 2012. FRET-based genetically encoded sensors allow high-resolution live cell imaging of Ca^{2+} dynamics. *Plant J.* 69:181–92
102. Krebs M, Schumacher K. 2013. Live cell imaging of cytoplasmic and nuclear Ca^{2+} dynamics in *Arabidopsis* roots. *Cold Spring Harb. Protoc.* 2013:776–80
103. Kudla J, Batistic O, Hashimoto K. 2010. Calcium signals: the lead currency of plant information processing. *Plant Cell* 22:541–63
104. Kuner T, Augustine GJ. 2000. A genetically encoded ratiometric indicator for chloride: capturing chloride transients in cultured hippocampal neurons. *Neuron* 27:447–59
105. Kwak JM, Mori IC, Pei ZM, Leonhardt N, Torres MA, et al. 2003. NADPH oxidase *AtrbohD* and *AtrbohF* genes function in ROS-dependent ABA signaling in *Arabidopsis. EMBO J.* 22:2623–33
106. Ladwig F, Stahl M, Ludewig U, Hirner AA, Hammes UZ, et al. 2012. *Siliques are Red1* from Arabidopsis acts as a bidirectional amino acid transporter that is crucial for the amino acid homeostasis of siliques. *Plant Physiol.* 158:1643–55
107. Lanquar V, Grossmann G, Vinkenborg JL, Merkx M, Thomine S, Frommer WB. 2014. Dynamic imaging of cytosolic zinc in *Arabidopsis* roots combining FRET sensors and RootChip technology. *New Phytol.* 202:198–208
108. Larrieu A, Champion A, Legrand J, Lavenus J, Mast D, et al. 2015. A fluorescent hormone biosensor reveals the dynamics of jasmonate signalling in plants. *Nat. Commun.* 6:6043
109. Lassig R, Gutermuth T, Bey TD, Konrad KR, Romeis T. 2014. Pollen tube NAD(P)H oxidases act as a speed control to dampen growth rate oscillations during polarized cell growth. *Plant J.* 78:94–106
110. Le J, Liu XG, Yang KZ, Chen XL, Zou JJ, et al. 2014. Auxin transport and activity regulate stomatal patterning and development. *Nat. Commun.* 5:3090

92. Describes a genetically encoded FRET biosensor (ABACUS1) for the stress hormone abscisic acid.

111. Lemke EA, Schultz C. 2011. Principles for designing fluorescent sensors and reporters. *Nat. Chem. Biol.* 7:480–83
112. Leran S, Varala K, Boyer JC, Chiurazzi M, Crawford N, et al. 2014. A unified nomenclature of NITRATE TRANSPORTER 1/PEPTIDE TRANSPORTER family members in plants. *Trends Plant Sci.* 19:5–9
113. Liao CY, Smet W, Brunoud G, Yoshida S, Vernoux T, Weijers D. 2015. Reporters for sensitive and quantitative measurement of auxin response. *Nat. Methods* 12:207–10
114. Litzlbauer J, Schifferer M, Ng D, Fabritius A, Thestrup T, Griesbeck O. 2015. Large scale bacterial colony screening of diversified FRET biosensors. *PLOS ONE* 10:e0119860
115. Loro G, Drago I, Pozzan T, Schiavo FL, Zottini M, Costa A. 2012. Targeting of Cameleons to various subcellular compartments reveals a strict cytoplasmic/mitochondrial Ca^{2+} handling relationship in plant cells. *Plant J.* 71:1–13
116. Loro G, Wagner S, Doccula FG, Behera S, Weinl S, et al. 2016. Chloroplast-specific in vivo Ca^{2+} imaging using Yellow Cameleon fluorescent protein sensors reveals organelle-autonomous Ca^{2+} signatures in the stroma. *Plant Physiol.* 171:2317–30
117. Luo Y, Scholl S, Doering A, Zhang Y, Irani NG, et al. 2015. V-ATPase activity in the TGN/EE is required for exocytosis and recycling in *Arabidopsis. Nat. Plants* 1:15094
118. Mank M, Santos AF, Direnberger S, Mrsic-Flogel TD, Hofer SB, et al. 2008. A genetically encoded calcium indicator for chronic in vivo two-photon imaging. *Nat. Methods* 5:805–11
119. Marchive C, Roudier F, Castaings L, Brehaut V, Blondet E, et al. 2013. Nuclear retention of the transcription factor NLP7 orchestrates the early response to nitrate in plants. *Nat. Commun.* 4:1713
120. Martiniere A, Bassil E, Jublanc E, Alcon C, Reguera M, et al. 2013. In vivo intracellular pH measurements in tobacco and *Arabidopsis* reveal an unexpected pH gradient in the endomembrane system. *Plant Cell* 25:4028–43
121. Marty L, Siala W, Schwarzlander M, Fricker MD, Wirtz M, et al. 2009. The NADPH-dependent thioredoxin system constitutes a functional backup for cytosolic glutathione reductase in *Arabidopsis. PNAS* 106:9109–14
122. Meyer AJ, Brach T, Marty L, Kreye S, Rouhier N, et al. 2007. Redox-sensitive GFP in *Arabidopsis thaliana* is a quantitative biosensor for the redox potential of the cellular glutathione redox buffer. *Plant J.* 52:973–86
123. Michard E, Lima PT, Borges F, Silva AC, Portes MT, et al. 2011. Glutamate receptor-like genes form Ca^{2+} channels in pollen tubes and are regulated by pistil D-serine. *Science* 332:434–37
124. Miesenbock G, De Angelis DA, Rothman JE. 1998. Visualizing secretion and synaptic transmission with pH-sensitive green fluorescent proteins. *Nature* 394:192–95
125. Mittler R. 2017. ROS are good. *Trends Plant Sci.* 22:11–19
126. Mittler R, Vanderauwera S, Gollery M, Van Breusegem F. 2004. Reactive oxygen gene network of plants. *Trends Plant Sci.* 9:490–98
127. Miyawaki A, Llopis J, Heim R, McCaffery JM, Adams JA, et al. 1997. Fluorescent indicators for Ca^{2+} based on green fluorescent proteins and calmodulin. *Nature* 388:882–87
128. Monshausen GB, Bibikova TN, Messerli MA, Shi C, Gilroy S. 2007. Oscillations in extracellular pH and reactive oxygen species modulate tip growth of *Arabidopsis* root hairs. *PNAS* 104:20996–1001
129. Monshausen GB, Bibikova TN, Weisenseel MH, Gilroy S. 2009. Ca^{2+} regulates reactive oxygen species production and pH during mechanosensing in *Arabidopsis* roots. *Plant Cell* 21:2341–56
130. Monshausen GB, Messerli MA, Gilroy S. 2008. Imaging of the Yellow Cameleon 3.6 indicator reveals that elevations in cytosolic Ca^{2+} follow oscillating increases in growth in root hairs of Arabidopsis. *Plant Physiol.* 147:1690–98
131. Monshausen GB, Miller ND, Murphy AS, Gilroy S. 2011. Dynamics of auxin-dependent Ca^{2+} and pH signaling in root growth revealed by integrating high-resolution imaging with automated computer vision-based analysis. *Plant J.* 65:309–18
132. Mori IC, Murata Y, Yang Y, Munemasa S, Wang YF, et al. 2006. CDPKs CPK6 and CPK3 function in ABA regulation of guard cell S-type anion- and Ca^{2+}-permeable channels and stomatal closure. *PLOS Biol.* 4:e327

133. Moseyko N, Feldman LJ. 2001. Expression of pH-sensitive green fluorescent protein in *Arabidopsis thaliana*. *Plant Cell Environ*. 24:557–63
134. Mukherjee P, Banerjee S, Wheeler A, Ratliff LA, Irigoyen S, et al. 2015. Live imaging of inorganic phosphate in plants with cellular and subcellular resolution. *Plant Physiol*. 167:628–38
135. Muller B, Fastner A, Karmann J, Mansch V, Hoffmann T, et al. 2015. Amino acid export in developing *Arabidopsis* seeds depends on UmamiT facilitators. *Curr. Biol.* 25:3126–31
136. Muller B, Sheen J. 2008. Cytokinin and auxin interaction in root stem-cell specification during early embryogenesis. *Nature* 453:1094–97
137. Munemasa S, Oda K, Watanabe-Sugimoto M, Nakamura Y, Shimoishi Y, Murata Y. 2007. The *coronatine-insensitive 1* mutation reveals the hormonal signaling interaction between abscisic acid and methyl jasmonate in Arabidopsis guard cells. Specific impairment of ion channel activation and second messenger production. *Plant Physiol*. 143:1398–407
138. Munnik T, Testerink C. 2009. Plant phospholipid signaling: "in a nutshell." *J. Lipid Res.* 50(Suppl.):S260–65
139. Murase K, Hirano Y, Sun TP, Hakoshima T. 2008. Gibberellin-induced DELLA recognition by the gibberellin receptor GID1. *Nature* 456:459–63
140. Nadler DC, Morgan SA, Flamholz A, Kortright KE, Savage DF. 2016. Rapid construction of metabolite biosensors using domain-insertion profiling. *Nat. Commun.* 7:12266
141. Nagai T, Sawano A, Park ES, Miyawaki A. 2001. Circularly permuted green fluorescent proteins engineered to sense Ca^{2+}. *PNAS* 98:3197–202
142. Nagai T, Yamada S, Tominaga T, Ichikawa M, Miyawaki A. 2004. Expanded dynamic range of fluorescent indicators for Ca^{2+} by circularly permuted yellow fluorescent proteins. *PNAS* 101:10554–59
143. Nakai J, Ohkura M, Imoto K. 2001. A high signal-to-noise Ca^{2+} probe composed of a single green fluorescent protein. *Nat. Biotechnol.* 19:137–41
144. Ngo QA, Vogler H, Lituiev DS, Nestorova A, Grossniklaus U. 2014. A calcium dialog mediated by the FERONIA signal transduction pathway controls plant sperm delivery. *Dev. Cell* 29:491–500
145. Novak O, Napier R, Ljung K. 2017. Zooming in on plant hormone analysis: tissue- and cell-specific approaches. *Annu. Rev. Plant Biol.* 68:323–48
146. O'Connor N, Silver RB. 2007. Ratio imaging: practical considerations for measuring intracellular Ca^{2+} and pH in living cells. *Methods Cell Biol*. 81:415–33
147. Okumoto S, Jones A, Frommer WB. 2012. Quantitative imaging with fluorescent biosensors. *Annu. Rev. Plant Biol.* 63:663–706
148. Oldroyd GE. 2013. Speak, friend, and enter: signalling systems that promote beneficial symbiotic associations in plants. *Nat. Rev. Microbiol.* 11:252–63
149. Ostergaard H, Henriksen A, Hansen FG, Winther JR. 2001. Shedding light on disulfide bond formation: engineering a redox switch in green fluorescent protein. *EMBO J*. 20:5853–62
150. Ottenschlager I, Wolff P, Wolverton C, Bhalerao RP, Sandberg G, et al. 2003. Gravity-regulated differential auxin transport from columella to lateral root cap cells. *PNAS* 100:2987–91
151. Palmer AE, Giacomello M, Kortemme T, Hires SA, Lev-Ram V, et al. 2006. Ca^{2+} indicators based on computationally redesigned calmodulin-peptide pairs. *Chem. Biol.* 13:521–30
152. Parton RM, Fischer-Parton S, Trewavas AJ, Watahiki MK. 2003. Pollen tubes exhibit regular periodic membrane trafficking events in the absence of apical extension. *J. Cell Sci.* 116:2707–19
153. Pei ZM, Murata Y, Benning G, Thomine S, Klusener B, et al. 2000. Calcium channels activated by hydrogen peroxide mediate abscisic acid signalling in guard cells. *Nature* 406:731–34
154. Perez Koldenkova V, Nagai T. 2013. Genetically encoded Ca^{2+} indicators: properties and evaluation. *Biochim. Biophys. Acta* 1833:1787–97
155. Peroza EA, Boumezbeur AH, Zamboni N. 2015. Rapid, randomized development of genetically encoded FRET sensors for small molecules. *Analyst* 140:4540–48
156. Persechini A, Lynch JA, Romoser VA. 1997. Novel fluorescent indicator proteins for monitoring free intracellular Ca^{2+}. *Cell Calcium* 22:209–16
157. Procko C, Burko Y, Jaillais Y, Ljung K, Long JA, Chory J. 2016. The epidermis coordinates auxin-induced stem growth in response to shade. *Genes Dev*. 30:1529–41

140. Describes a novel strategy for the screening of cpGFP insertion sites into ligand-binding domains using a combination of transposon-based cloning, fluorescence-activated cell sorting, and next-generation sequencing.

144. Describes the first multicolor calcium imaging approach to simultaneously visualize calcium signals in pollen tubes and synergids during double fertilization in *Arabidopsis*.

158. Richmond TA, Takahashi TT, Shimkhada R, Bernsdorf J. 2000. Engineered metal binding sites on green fluorescence protein. *Biochem. Biophys. Res. Commun.* 268:462–65
159. Rincon-Zachary M, Teaster ND, Sparks JA, Valster AH, Motes CM, Blancaflor EB. 2010. Fluorescence resonance energy transfer-sensitized emission of yellow cameleon 3.60 reveals root zone-specific calcium signatures in Arabidopsis in response to aluminum and other trivalent cations. *Plant Physiol.* 152:1442–58
160. Rizza A, Walia A, Lanquar V, Frommer WB, Jones AM. 2017. In vivo gibberellin gradients visualized in rapidly elongating tissues. *Nat Plants* 3:803–13
161. Rosa S, De Lucia F, Mylne JS, Zhu D, Ohmido N, et al. 2013. Physical clustering of *FLC* alleles during Polycomb-mediated epigenetic silencing in vernalization. *Genes Dev.* 27:1845–50
162. Rose T, Goltstein PM, Portugues R, Griesbeck O. 2014. Putting a finishing touch on GECIs. *Front. Mol. Neurosci.* 7:88
163. Rosenwasser S, Rot I, Meyer AJ, Feldman L, Jiang K, Friedman H. 2010. A fluorometer-based method for monitoring oxidation of redox-sensitive GFP (roGFP) during development and extended dark stress. *Physiol. Plant* 138:493–502
164. Sabatini S, Beis D, Wolkenfelt H, Murfett J, Guilfoyle T, et al. 1999. An auxin-dependent distal organizer of pattern and polarity in the *Arabidopsis* root. *Cell* 99:463–72
165. Sadanandom A, Napier RM. 2010. Biosensors in plants. *Curr. Opin. Plant Biol.* 13:736–43
166. Samodelov SL, Beyer HM, Guo X, Augustin M, Jia KP, et al. 2016. StrigoQuant: a genetically encoded biosensor for quantifying strigolactone activity and specificity. *Sci. Adv.* 2:e1601266
167. Sato EM, Hijazi H, Bennett MJ, Vissenberg K, Swarup R. 2015. New insights into root gravitropic signalling. *J. Exp. Bot.* 66:2155–65
168. Sauret-Gueto S, Calder G, Harberd NP. 2012. Transient gibberellin application promotes *Arabidopsis thaliana* hypocotyl cell elongation without maintaining transverse orientation of microtubules on the outer tangential wall of epidermal cells. *Plant J.* 69:628–39
169. Schulte A, Lorenzen I, Bottcher M, Plieth C. 2006. A novel fluorescent pH probe for expression in plants. *Plant Methods* 2:7
170. Schumacher K. 2014. pH in the plant endomembrane system: an import and export business. *Curr. Opin. Plant Biol.* 22:71–76
171. Schumacher K, Vafeados D, McCarthy M, Sze H, Wilkins T, Chory J. 1999. The *Arabidopsis det3* mutant reveals a central role for the vacuolar H^+-ATPase in plant growth and development. *Genes Dev.* 13:3259–70
172. Schuster C, Gaillochet C, Medzihradszky A, Busch W, Daum G, et al. 2014. A regulatory framework for shoot stem cell control integrating metabolic, transcriptional, and phytohormone signals. *Dev. Cell* 28:438–49
173. Schwarzlander M, Fricker MD, Muller C, Marty L, Brach T, et al. 2008. Confocal imaging of glutathione redox potential in living plant cells. *J. Microsc.* 231:299–316
174. Shaner NC, Patterson GH, Davidson MW. 2007. Advances in fluorescent protein technology. *J. Cell Sci.* 120:4247–60
175. Shaner NC, Steinbach PA, Tsien RY. 2005. A guide to choosing fluorescent proteins. *Nat. Methods* 2:905–9
176. Shen J, Zeng Y, Zhuang X, Sun L, Yao X, et al. 2013. Organelle pH in the *Arabidopsis* endomembrane system. *Mol. Plant* 6:1419–37
177. Shih HW, DePew CL, Miller ND, Monshausen GB. 2015. The cyclic nucleotide-gated channel CNGC14 regulates root gravitropism in *Arabidopsis thaliana*. *Curr. Biol.* 25:3119–25
178. Sieberer BJ, Chabaud M, Fournier J, Timmers AC, Barker DG. 2012. A switch in Ca^{2+} spiking signature is concomitant with endosymbiotic microbe entry into cortical root cells of *Medicago truncatula*. *Plant J.* 69:822–30
179. Sieberer BJ, Chabaud M, Timmers AC, Monin A, Fournier J, Barker DG. 2009. A nuclear-targeted cameleon demonstrates intranuclear Ca^{2+} spiking in *Medicago truncatula* root hairs in response to rhizobial nodulation factors. *Plant Physiol.* 151:1197–206
180. Silverstone AL, Tseng TS, Swain SM, Dill A, Jeong SY, et al. 2007. Functional analysis of SPINDLY in gibberellin signaling in Arabidopsis. *Plant Physiol.* 143:987–1000

160. Describes a high-affinity FRET biosensor used to report on the levels of gibberellin in plant tissues.

181. Simon ML, Platre MP, Assil S, van Wijk R, Chen WY, et al. 2014. A multi-colour/multi-affinity marker set to visualize phosphoinositide dynamics in Arabidopsis. *Plant J*. 77:322–37
182. Sozzani R, Busch W, Spalding EP, Benfey PN. 2014. Advanced imaging techniques for the study of plant growth and development. *Trends Plant Sci*. 19:304–10
183. Steinhorst L, Kudla J. 2013. Calcium - a central regulator of pollen germination and tube growth. *Biochim. Biophys. Acta* 1833:1573–81
184. Stepanova AN, Yun J, Likhacheva AV, Alonso JM. 2007. Multilevel interactions between ethylene and auxin in *Arabidopsis* roots. *Plant Cell* 19:2169–85
185. Suzuki J, Kanemaru K, Ishii K, Ohkura M, Okubo Y, Iino M. 2014. Imaging intraorganellar Ca^{2+} at subcellular resolution using CEPIA. *Nat. Commun.* 5:4153
186. Swarup K, Benkova E, Swarup R, Casimiro I, Peret B, et al. 2008. The auxin influx carrier LAX3 promotes lateral root emergence. *Nat. Cell Biol.* 10:946–54
187. Tang S, Wong HC, Wang ZM, Huang Y, Zou J, et al. 2011. Design and application of a class of sensors to monitor Ca^{2+} dynamics in high Ca^{2+} concentration cellular compartments. *PNAS* 108:16265–70
188. Thestrup T, Litzlbauer J, Bartholomaus I, Mues M, Russo L, et al. 2014. Optimized ratiometric calcium sensors for functional in vivo imaging of neurons and T lymphocytes. *Nat. Methods* 11:175–82
189. Thor K, Peiter E. 2014. Cytosolic calcium signals elicited by the pathogen-associated molecular pattern flg22 in stomatal guard cells are of an oscillatory nature. *New Phytol*. 204:873–81
190. Tian L, Hires SA, Mao T, Huber D, Chiappe ME, et al. 2009. Imaging neural activity in worms, flies and mice with improved GCaMP calcium indicators. *Nat. Methods* 6:875–81
191. Ulmasov T, Murfett J, Hagen G, Guilfoyle TJ. 1997. Aux/IAA proteins repress expression of reporter genes containing natural and highly active synthetic auxin response elements. *Plant Cell* 9:1963–71
192. Uslu VV, Grossmann G. 2016. The biosensor toolbox for plant developmental biology. *Curr. Opin. Plant Biol.* 29:138–47
193. Vermeer JE, Munnik T. 2013. Using genetically encoded fluorescent reporters to image lipid signalling in living plants. *Methods Mol. Biol.* 1009:283–89
194. Vermeer JE, Thole JM, Goedhart J, Nielsen E, Munnik T, Gadella TW Jr. 2009. Imaging phosphatidylinositol 4-phosphate dynamics in living plant cells. *Plant J*. 57:356–72
195. Vinkenborg JL, Nicolson TJ, Bellomo EA, Koay MS, Rutter GA, Merkx M. 2009. Genetically encoded FRET sensors to monitor intracellular Zn^{2+} homeostasis. *Nat. Methods* 6:737–40
196. von Wiren N, Gazzarrini S, Gojon A, Frommer WB. 2000. The molecular physiology of ammonium uptake and retrieval. *Curr. Opin. Plant Biol.* 3:254–61
197. Waadt R, Hitomi K, Nishimura N, Hitomi C, Adams SR, et al. 2014. FRET-based reporters for the direct visualization of abscisic acid concentration changes and distribution in Arabidopsis. *eLife* 3:e01739
198. Waadt R, Hsu PK, Schroeder JI. 2015. Abscisic acid and other plant hormones: methods to visualize distribution and signaling. *Bioessays* 37:1338–49
199. Waadt R, Krebs M, Kudla J, Schumacher K. 2017. Multiparameter imaging of calcium and abscisic acid and high-resolution quantitative calcium measurements using R-GECO1-mTurquoise in Arabidopsis. *New Phytol*. 216:303–20
200. Wachter RM, Remington SJ. 1999. Sensitivity of the yellow variant of green fluorescent protein to halides and nitrate. *Curr. Biol.* 9:R628–29
201. Wagner S, Behera S, De Bortoli S, Logan DC, Fuchs P, et al. 2015. The EF-hand Ca^{2+} binding protein MICU choreographs mitochondrial Ca^{2+} dynamics in Arabidopsis. *Plant Cell* 27:3190–212
202. Wang YF, Munemasa S, Nishimura N, Ren HM, Robert N, et al. 2013. Identification of cyclic GMP-activated nonselective Ca^{2+}-permeable cation channels and associated *CNGC5* and *CNGC6* genes in Arabidopsis guard cells. *Plant Physiol*. 163:578–90
203. Weinl S, Held K, Schlucking K, Steinhorst L, Kuhlgert S, et al. 2008. A plastid protein crucial for Ca^{2+}-regulated stomatal responses. *New Phytol*. 179:675–86
204. Wells DM, Laplaze L, Bennett MJ, Vernoux T. 2013. Biosensors for phytohormone quantification: challenges, solutions, and opportunities. *Trends Plant Sci*. 18:244–49
205. Wrzaczek M, Brosche M, Kangasjarvi J. 2013. ROS signaling loops: production, perception, regulation. *Curr. Opin. Plant Biol.* 16:575–82

197. Describes a genetically encoded FRET biosensor (ABAleon2.1) for the stress hormone abscisic acid.

206. Xue S, Hu H, Ries A, Merilo E, Kollist H, Schroeder JI. 2011. Central functions of bicarbonate in S-type anion channel activation and OST1 protein kinase in CO_2 signal transduction in guard cell. *EMBO J.* 30:1645–58
207. Yang H, Bogner M, Stierhof YD, Ludewig U. 2010. H-independent glutamine transport in plant root tips. *PLOS ONE* 5:e8917
208. Ye W, Muroyama D, Munemasa S, Nakamura Y, Mori IC, Murata Y. 2013. Calcium-dependent protein kinase CPK6 positively functions in induction by yeast elicitor of stomatal closure and inhibition by yeast elicitor of light-induced stomatal opening in Arabidopsis. *Plant Physiol.* 163:591–99
209. Young JJ, Mehta S, Israelsson M, Godoski J, Grill E, Schroeder JI. 2006. CO_2 signaling in guard cells: calcium sensitivity response modulation, a Ca^{2+}-independent phase, and CO_2 insensitivity of the *gca2* mutant. *PNAS* 103:7506–11
210. Yuan F, Yang H, Xue Y, Kong D, Ye R, et al. 2014. OSCA1 mediates osmotic-stress-evoked Ca^{2+} increases vital for osmosensing in *Arabidopsis*. *Nature* 514:367–71
211. Zhao Y, Araki S, Wu J, Teramoto T, Chang YF, et al. 2011. An expanded palette of genetically encoded Ca^{2+} indicators. *Science* 333:1888–91
212. Zhu Q, Wang L, Dong Q, Chang S, Wen K, et al. 2017. FRET-based glucose imaging identifies glucose signalling in response to biotic and abiotic stresses in rice roots. *J. Plant Physiol.* 215:65–72
213. Zurcher E, Tavor-Deslex D, Lituiev D, Enkerli K, Tarr PT, Muller B. 2013. A robust and sensitive synthetic sensor to monitor the transcriptional output of the cytokinin signaling network *in planta*. *Plant Physiol.* 161:1066–75
214. Ishitani M, Xiong L, Stevenson B, Zhu JK. 1997. Genetic analysis of osmotic and cold stress signal transduction in *Arabidopsis thaliana*: interactions and convergence of abscisic acid-dependent and abscisic acid-independent pathways. *Plant Cell* 9:1935–49
215. Kim TH, Hauser F, Ha T, Xue S, Böhmer M, et al. 2011. Chemical genetics reveals negative regulation of abscisic acid signaling by a plant immune response pathway. *Curr. Biol.* 21:990–97

211. Describes the development of genetically encoded calcium indicators for optical imaging (GECOs) that emit fluorescence at various wavelengths.